THE UNIVERSITY OF QUEENSLAND

Bachelor of Engineering Thesis Report

Influence of Alloy Parameters and Testing Conditions on Performance of White Cast Irons in the Ball Mill Abrasion Test

Student Name: George Galis

Course Code: MECH4501

Supervisor: Mr Hamid Pourasiabi / Dr Jeff Gates

Submission date: 30 May 2019

UQ Engineering

Faculty of Engineering, Architecture and Information Technology

This page is left intentionally blank

Acknowledgements

I would like to give thanks to the UQMP team especially Hamid and Jeff, my peers Sharifah and Carlos in the other UQMP projects and Phil Bennet and Lenny McInnes for all the training on various equipment and forklift assistance. To Rowan James Conaghan, for his advice and wisdom on the conduction, writing and logistics of theses.

To E.J.W. and W.H.H. for being large parts of my life during the conduction of my thesis.

Abstract

The Ball Mill Abrasion Test (BMAT) is a wear test that employs a tumbling mill with balls and edge-rounded block specimens of selected alloys. This project examines the performance of a range of high chromium white cast iron samples with varying alloy composition. White cast iron is a particle-reinforced composite whereby very hard carbide phases are surrounded by a moderately hard but relatively tough (fracture-resistant) martensitic matrix.

This project sets out to understand the factors affecting the ability of high chromium white cast irons to provide superior wear life compared with steels. The project investigates which compositions of white cast iron performs best in industrial wear applications such as ball mills. This has been investigated by varying the key alloy parameters carbide volume fraction (CVF) and chromium to carbon ratio (Cr:C), and investigating their effects under a range of testing conditions.

Reviewing literature, a knowledge gap was identified of the exact effects of CVF and Cr:C. These parameters have been observed to have either positive or negative impacts on wear life depending on test conditions.

The alloys selected for the experimental program had systematically varied CVF and Cr:C, organised into series where the opposing variable is kept approximately constant. In addition, a selection of common abrasion resistant steels were included. In order to determine the benefits of white cast irons and the effects of the alloy parameters, the BMAT was employed. Various testing conditions were employed, to determine whether alloy parameters had differing effects under the different conditions. The test parameters varied included: abrasive type, abrasive feed particle size distribution, and test duration.

Specific combinations of the conditions were determined by an edited version of the optimal Design of Experiment (DoE) method, which allows for conclusions to be drawn without having to complete full factorial experiments (which could not be completed under time constraints).

The testing determined that:

(1) The magnitude of benefit of white cast irons compared to low-alloy steels is largest when tested in softer abrasives. This is consistent with past publications.

(2) For a given abrasive rock type, the magnitude of benefit of white cast irons was greater for larger feed particle size. This is contrary to the findings of past experimental work.

(3) Carbide volume fraction did not show a clear effect on wear performance. This is reasonably consistent with past work, which has shown only weak (and somewhat variable) effects of CVF on abrasion performance under high stress abrasion conditions.

(4) Increasing chromium to carbon ratio was found to have a negative effect on abrasive wear life, although it may benefit corrosion resistance.

(5) An alloy denoted Y062 (medium range CVF of 34.6 vol% and the medium Cr:C ratio of 5.3) showed the best wear performance averaged over all wear conditions.

Recommendations for future testing include more testing with BMAT with gaps between particle size distribution to highlight the effect of sized. Alternatively, within these distributions ensuring fair spread of sizes as the makeup within these ranges as it was not exactly known.

Table of Contents

List of figures

List of Tables

Abbreviations

BMAT: Ball Mill Abrasion Test

BMECT: Ball Mill Edge Chipping Test

ICAT: Inner Circumference Abrasion Test

IC-SBAT: Inner Circumference Sliding Bed Abrasion Test

RWAT: Rubber Wheel Abrasion Test

DS-RWAT: Dry Sand – Rubber Wheel Abrasion Test

WCI: White Cast Iron

CVF: Carbide Volume Fraction

Cr:C : Chromium To Carbon Ratio

CVF(E): Effective Carbide Volume Fraction

Cr(E):C :Effective Chromium To Carbon Ratio

UQMP: UQ Materials Performance

This page is left intentionally blank

1.0 Introduction

1.1 Background

This project is one of a three-part overarching project being conducted Aug 2018-May 2019, and also building upon work performed in previous years. This thesis will specifically outline the Influence of Alloy Parameters and Testing Conditions on Performance of White Cast Irons in the Ball Mill Abrasion Test. It will build on the past knowledge found in the Osaka experiments (Gates, et al., 2017) which were previous tests completed by UQMP that tested other parameters of white cast irons in a range of test types.

White cast iron is a particle-reinforced composite alloy whereby a relatively soft matrix comparable to low alloy martensitic steel is combined with a significantly harder phase made of a combination of carbides which vary upon composition.

The ball mill abrasion test (BMAT) employs the use of a tumbling mill with balls of a selected alloy. It produces conditions that are much more similar to industry applications of ball mills when compared to conventional laboratory wear tests. Errors in the prediction of industrial service performance based on laboratory test data are due to current methods of wear research not producing correct wear mechanisms.

The specimens to be used in this project are rectangular blocks with rounded edges and corners.

1.2 Thesis Aim and Motivation

This project sets out to evaluate the influences of various test parameters on the performance of various compositions of high chromium white cast iron relative to steels. To determine factors that improve wear resistance and the magnitude of these benefits. (a) Alloy composition affects microstructure, which in turn influences resistance to abrasive wear. (b) White cast irons are particle-reinforced composites and this type of microstructure typically gives better abrasive wear resistance than homogenous steels; but among white cast irons, some have better

wear-resistance than others. (c) This project aims to quantify the effects of key microstructural parameters on wear performance of white cast irons, notably carbide volume fraction and chrome to carbon ratio. (d) In addition, the project aims to check whether these performance trends are sensitive to the details of the abrasive environment, such as the abrasive mineral type or particle size.

The goal is to produce enough data to draw conclusions on the viability of white cast iron provide a better wear life when compared with steels and further, what composition of white cast iron performs the best. This will allow for a recommendation to be made to industry on the implementation the use of white cast iron in high wear applications.

1.3 Strategy

To determine the relative wear performance of different alloys under various conditions, the BMAT will be used. The wear rates will be measured for a set of specimens of alloys with systematically varying parameters, with all alloys being subjected to the wear environment simultaneously.

Using samples from the 2017 Osaka experiment a past UQMP test conducted by Gates et al. along with additional steel specimens, a wide collection of samples will be tested utilising the BMAT. The samples have varying carbide volume fraction (CVF) and chromium to carbon ratio (Cr:C). These will be tested over periods of a few hours and then mass loss will be calculated. Then the mass losses of the different alloys will be compared to determine which alloys are more wear resistant.

Such tests will be repeated using a variety of different abrasives and in multiple feed particle size distributions and Durations.

1.4 Scope

Table 1: Scope of thesis

In Scope	Out of Scope
Systematic experiments on effects CVF and Cr:C.	Intentional variation of other materials properties.
A range of environmental parameters as outlined in 3.1.1	Environmental parameters of the BMAT not outlined in 3.1.1
Consideration of bulk Vickers hardness	Micro-hardness of specific phases of the white cast irons such as the carbides

1.5 Hypotheses

Firstly, it is expected that for most industrially-realistic conditions, white cast iron will perform better than steel in the high wear situations.

In regards to higher carbide volume fraction, it is predicted that the presence of harder phases will assist wear resistance as they obstruct the wear of the matrix given their significantly higher hardness. Thus the presence of a higher volume fraction of the harder carbide should therefore decrease wear rate.

In regards to higher Cr:C, with more chromium it is expected the matrix will become more corrosion resistant, hence if corrosion is a significant contributing wear mechanism then increased Cr:C might be expected to increase the wear performance. However, increase in Cr:C ratio is known to decrease the carbon content of the martensite matrix, which reduces its hardness; hence if corrosion is not a significant contributing wear mechanism then increasing Cr:C ratio might therefore reduce wear performance.

In regards to the effect of the abrasive minerals used, it is expected that the effectiveness of the carbides in providing wear resistance will decrease when harder, stronger abrasives are used, because harder stronger minerals are more likely to fracture the carbides so that they can no

longer protect the matrix. Giving performance comparable to as competence of the mineral is increased.

In regards to the effect of duration, as duration of test is extended, the final particle size is reduced, meaning while at the start of testing the particles will be course enough to break the carbides, once these particles are crushed, the white cast iron should perform better.

Finally, in regards to abrasive particle size, it is expected that larger particles will be more likely to fracture the carbides so that they can no longer protect the matrix, hence the relative performance of white cast irons will be poorer for large abrasive particles.

2.0 Literature Review

2.1 Archard Wear Equation.

The Archard wear equation is was developed as a theoretical basis to explain the wear of materials (Archard & Hirst, 1956). It is used to find the worn volume of a sample undergoing abrasive wear.

$$W = k_1 \times k_2 \times \frac{F_n v_t}{H}$$

Where

W = worn volume

$k_1 = \tan\left(\frac{\phi}{\pi}\right)$ Angularity

$k_2 = \frac{V_\alpha}{V_g}$ = Wear Mechanism

F_n = Normal Force

v_t = Sliding Velocity

H = Hardness of softest material

v_α = Volume of wear debris

v_g = Volume of groove

2.2 Abrasive Wear Mechanisms

The major mechanisms involved in abrasive wear are displayed in Figure 1. Micro-ploughing, micro-cutting, micro-fatigue and micro-cracking are the key wear mechanisms outlined by Zum Gahr.

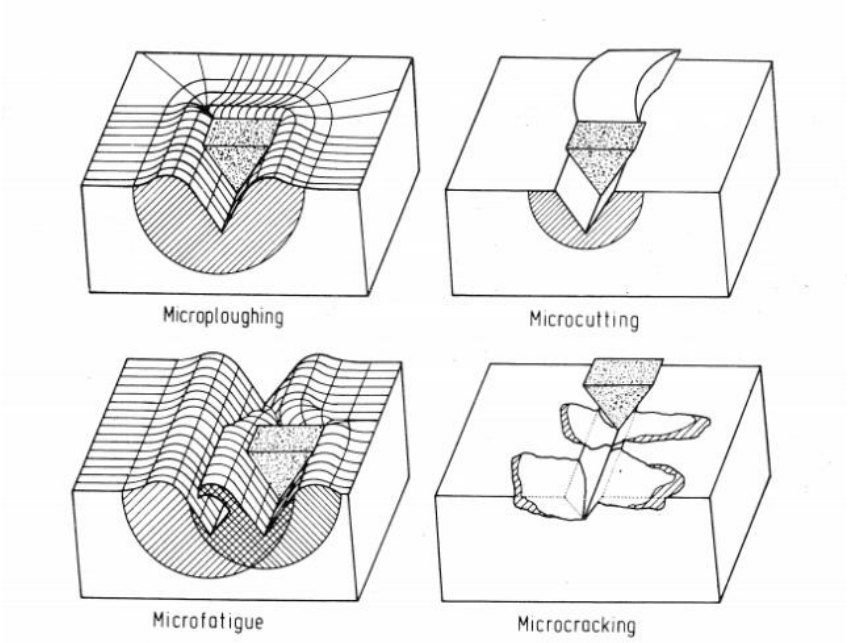

Figure 1: Physical interactions between abrasive particles and surface of materials (Zum Gahr, 1987)

Micro ploughing is the ideal mechanism that damages surfaces the least as it involves plastic deformation by the abrasive of the surface of the material, meaning mass is not necessarily lost in the process. It is only when multiple abrasive particles are ploughing aside consistently that particles will be worn away. (Zum Gahr, 1987). The volume of the wear debris is significantly less that the volume of the groove created, this inherently gives micro ploughing a low k_2 value between 0.01 – 0.1 (Gates & Gore, 1995)

Micro cutting is when the abrasive particles dig into the surface material which detaches the material unlike the deformation present in micro ploughing. Material lost is the majority of the volume of the gouge created giving micro cutting k_2 value between 0.2 – 1 (regularly 0.8) (Gates & Gore, 1995).

Micro cracking or micro fracture involves the brittle failure of the surface of the material resulting in large wear debris and is due to highly concentrated stresses applied by the abrasive particles (Zum Gahr, 1987). This is often due to micro cutting and additional material is lost by initiation and linkage of brittle cracks. As the wear debris is large, the volume of the debris is greater than the groove volume, giving micro cracking a $k_2 > 1$ (Gates & Gore, 1995).

2.3 Past Laboratory Testing

Work originally from Zum Gahr, K. H., 1987. Microstructure and Wear of Materials. Elsevier, as cited in Friction and Wear of Engineering Materials, Hutchings & Shipway 2017. An historic example of abrasion testing seen in Figure 2.

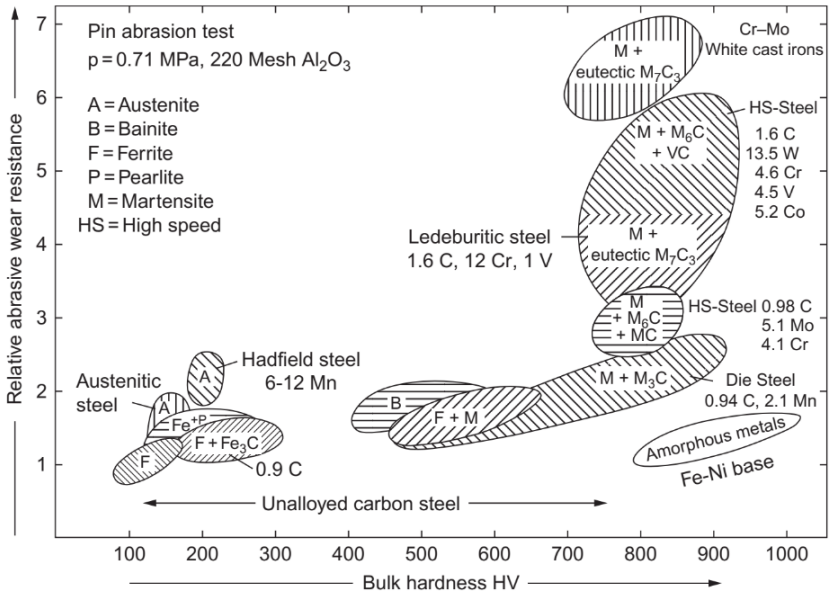

Figure 2: Effect of microstructure and composition on the relative two-body abrasive wear resistance of steels and cast irons against 70μm alumina particles (Zum Gahr, 1987).

Under theses testing conditions it is noted the significant benefit of white cast irons over various types of steel. However the pin abrasion test used in this testing has questionable reliability due to the abrasive wear mechanism not being representative of industrial ball mill conditions.

Peng, et al. investigated friction and wear of ball mill liners. The operating principle of the ball mill is shown in Figure 3

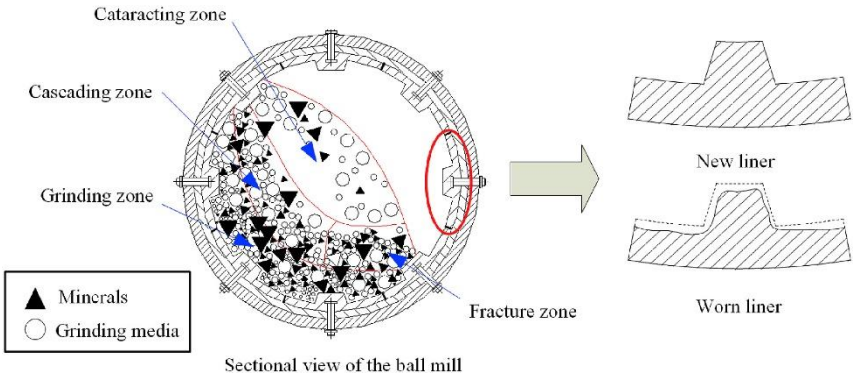

Figure 3: Working principle of Ball Mill

It is noted that damage to the liner and grinding media occurs when the mill speed is sufficient to allow cataracting, at the point where the minerals and grinding media impact the mill. To test the abrasion of the balls, a friction test rig whereby a single ball was rotated against a fixed plate as an alternative to pin on disk tribometer. It was concluded that this ball-cratering method of friction and wear testing at applying wear mechanism of grinding media and liners (Peng, et al., 2017). However as no abrasive is present this test only showed the effects of metal to metal sliding wear. This doesn't provide an accurate account of abrasive wear mechanisms, and these other mechanisms of wear that occur in a tumbling mill, as they cannot occur without the abrasive itself.

Heino, Kallio, Valtonen, & Kuokkala using the crushing pin on disc method tested high stress abrasion resistance of WCI. They concluded about austenite-to-martensite ratio while the martensite benefits hardness, overly high content leads to the matrix surface being prone to fracture. The carbides that form the columnar structure are most beneficial to abrasion resistance when orthogonal to the wear surface for the conditions tested. Predominantly the abrasion resistance of white cast irons is highly dependent on the wear conditions present and the properties and microstructure of the material. (Heino, Kallio, Valtonen, & Kuokkala, 2017)

2.3.1 Past Theses

Marnane, while investigating Ni-Hard 4 and high-Cr-Mo white case irons use of The Rubber Wheel Abrasion Test (RWAT) and Inner Circumference Abrasion Test (ICAT). These provided conflicting information and limited data on the abrasion resistance of the tested alloys in his project. Despite this it was concluded the high-Cr-Mo Alloys had superior wear resistance due to their higher CVF and harder carbide phases. (Marnane, 2018)

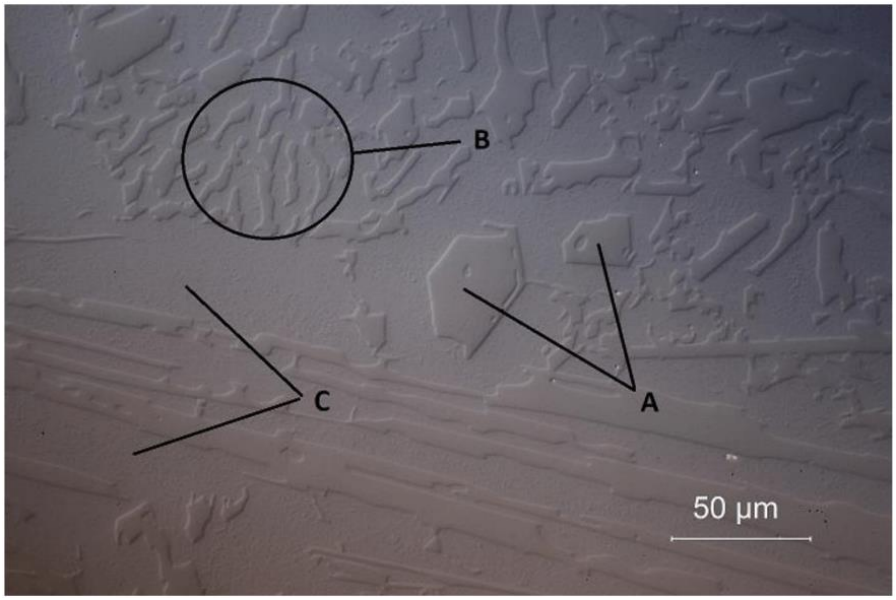

Figure 4: CB100 hyper-eutectic microstructure showing primary carbides and M_7C_3 eutectic, 50x magnification (Marnane, 2018)

Figure 4 shows a micrograph of the Alloy CB100 taken by Marnane, it highlights the key features of high chromium white cast namely:

(A) Primary M_7C_3 carbides
(B) M_7C_3 eutectic
(C) Iron rich matrix within the eutectic

Chen using dry sand rubber wheel abrasion test (DS-RWAT) and BMAT, varied CVF and CrE:C for his testing. It was found that CVF and CrE:C have a greater impact on low stress sliding abrasion relative to high normal stress abrasion. (Chen, 2018)

Another type of testing done was Ball Mill Edge Chipping Test (BMECT) as utilised by Hamzah in addition to BMAT. It was concluded that that a combination of low Cr:C and high CVF produced the optimum combination for lowest wear within the scope of the conditions tested. It was also found that High-Cr white cast irons performed better that Ni-Hard 4 but Ni-Hard 4 can be produced to have comparable performance. (Hamzah, 2018)

Comino using 300mm and 500mm BMAT and varying the angle of impingement (therefore increasing the impact), found that there was an increase in relative wear loss with increasing impact. Conversely the results were not conclusive as many of the samples didn't follow this trend (Comino, 2009).

Further when testing 600mm BMAT, the opposite of the expected trend was observed whereby the increasing impact the weight loss was less than that of the low stress abrasion (Comino, 2009).

By varying feed material in the high and low impact, it was observed that with the softer Cadia ore, there was a decrease in wear rate with an increase in CVF. With the harder quartz, a different trend was observed. Under the low speed testing, an increase in relative wear loss with an increase of CVF and a negligible difference for the higher speed was observed. (Comino, 2009) This could be due to the surrounding matrix being worn leaving the carbides exposed and then susceptible to fracturing.

According to Littler the relative performance benefit of white cast irons when compared to average wear rate of steel was observed to be 2.0 times superior, indicating that the wear rate at its maximum was still half of that of the average steel alloy. The use of the BMAT produced

conclusive results on the benefits of white cast irons within the scope of conditions tested. (Littler, 2015)

2.3.2 Osaka Project

The Osaka Project was a conference paper titled Understanding the Performance of Abrasion-resistant High-Cr White Cast Irons in Terms of Micro-, Meso- and Macro-scale Fracture Mechanisms. This project investigated various damage mechanisms which can impact the performance benefit of high chromium white cast irons over wear resistant steels.

This paper explores the damage mechanisms which can prevent achievement of the desired performance benefit which relies on the reinforcing composite not undergoing fracture-related damage mechanisms that the brittle carbides are prone to. The micro scale particularly pertains to this report (Gates, et al., 2017). The specimens used in the Osaka project were reused in the conduction of this project.

The paper found the effect of increasing CVF in low stress sliding abrasion to be highly beneficial, conversely in high normal stress abrasion, little benefit was noted. When changing from 18 to ~33 vol% the effect was only slight benefit was noted. A dramatic drop off was found when above 38 vol% presumed to be caused by micro-fracture wear mechanisms (Gates, et al., 2017).

In regards to the effect of Cr:C, increasing the matrix carbon content is somewhat beneficial under low stress abrasion such as the RWAT, conversely in high stress abrasion conditions such as in the Inner Circumference Sliding Bed Abrasion Test (IC-SBAT) decreasing Cr:C by increasing C content is disadvantageous as the micro-facture wear mechanisms become more prevalent in the more brittle microstructures (Gates, et al., 2017).

2.4 Knowledge Gap

The primary identified knowledge gap was with the effect of the carbide volume fraction.

Firstly, it has been observed in past theses such as Comino that, in the BMAT, varying the carbide volume fraction appears to have only a very weak effect on the performance of the alloys. In fact, contrary to the predictions of most literature on abrasive wear, results from the BMAT have sometimes found that increasing CVF leads to an increase in wear rate . Although such counter-intuitive behaviour has been observed in the past, it is not so well documented as to be regarded as routine knowledge; it still requires verification and more detailed study.

Secondly, past studies have provided little if any information about the effect of very low values of CVF. In fact the past data contain what appears to be a contradiction. It is almost always found (e.g. Littler) that white cast irons perform better than homogeneous steels. Since steels can be considered to be like the limiting case of a white cast iron with a CVF of zero, the observed negative effect of increasing CVF seems difficult to understand. The suggestion is that the curve of wear rate versus CVF might contain a minimum point and slope reversal; but if so, this minimum point must be at a value of CVF below what has been tested to date. Therefore, there is considerable interest in extending the performance data down to lower values of CVF, ideally to zero.

Additionally, there is very little systematic data for the effect of Cr:C ratio. Literature seems to suggest that reducing Cr:C ratio should imp rove abrasion resistance because it leads to higher-carbon martensite in the matrix, but this is not backed by hard data and especially not in high stress abrasion. Therefore there is considerable interest in generating systematic data for the effect of Cr:C in the BMAT.

3.0 Experimental Design

3.1 Methodology

3.1.1 Test Matrix

Table 2 below shows the range of testing conditions that were evaluated. It also shows the coding factors used for the design of experiment in section 3.1.3 The feed particle size range is an upper and lower limit on the size of the abrasive particles prior to testing.

Table 2: Test Matrix

Parameter	Selection 1 (-1)	Selection 2 (0)	Selection 3 (+1)
Abrasive Type	Basalt	Granite	Quartzite
Feed Particle Size Range (mm)	1.7 – 5.6	5.6 – 9.50	9.50 – 13.2
Test Duration	Short (5hr)	N/A	Long (25hr)

Basalt was sourced through a landscaping company from Mt. Morrow quarry, granite from Bracalaba and quartzite from Tumbulgum quarry

3.1.2 Mill Parameters

The mill used has a diameter of 600mm. Rotation speed used was determined from other tests completed by other undergraduate students and UQMP tests, an optimal speed of 55% of critical speed of the mill (21.33Hz for motor used in testing) whereby critical speed is the centrifuging speed. Make up charge used was Mag B with 25mm diameter.

Due to the large number of specimens, not all could be tested at once, as they would fill the mill over the preferred level of 45%. As a result, they were divided into two batches that could both be tested with the same conditions. Three specimen types, two located at key points on the phase diagram in Figure 6 and a steel were selected to be in both batches, these reference materials had 12 blocks each, and wear rates could be compared between batches.

3.1.3 Design of Experiment

Specific combinations of the conditions to be tested were determined by an optimal Design of Experiment method, which allows for conclusions to be drawn without having to complete full factorial experiments given time constraints. So in place of 18 tests, there are 11, 3 of which were repeated to show the reliability of the data shown by the highlighted cells. Test tests are shown below in Table 3.

Table 3: Experimental Design

Run Order #	Coded Factors			Factors		
	Abrasive Type	Feed PSD	Test Duration	Abrasive Type	Feed PSD	Test Duration
1	-1	-1	-1	Basalt	Fine	Short
2	-1	0	-1	Basalt	Medium	Short
3	-1	1	-1	Basalt	Coarse	Short
4	-1	1	-1	Basalt	Coarse	Short
5	-1	1	1	Basalt	Coarse	Long
6	0	0	-1	Granite	Medium	Short
7	0	0	-1	Granite	Medium	Short
8	0	1	-1	Granite	Coarse	Short
9	0	1	1	Granite	Coarse	Long
10	0	1	1	Granite	Coarse	Long
11	1	-1	-1	Quartzite	Fine	Short
12	1	0	-1	Quartzite	Medium	Short
13	1	1	-1	Quartzite	Coarse	Short
14	1	1	1	Quartzite	Coarse	Long

To visually represent the coded tests, Figure 5 shows the full factorial tests as the black dots, blue are tests completed and red are tests with replicates. The number of long test were minimised due to the practical limitations of time required.

.

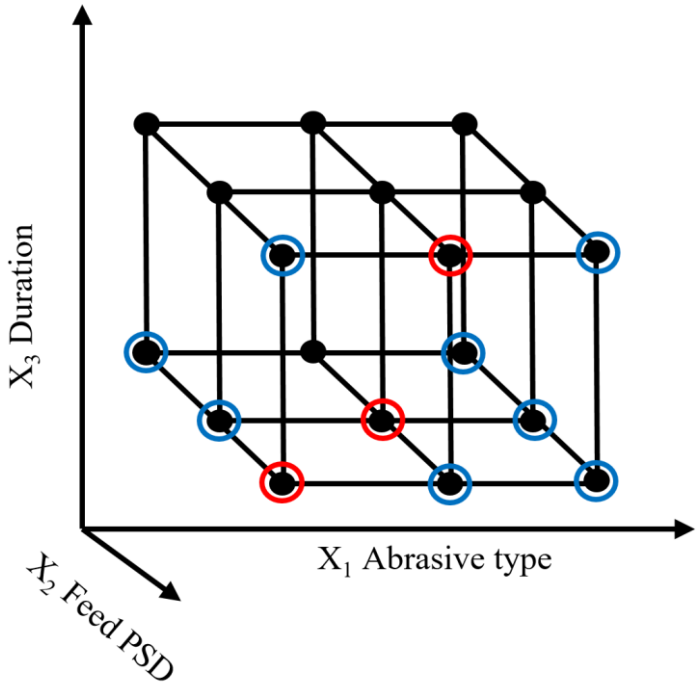

Figure 5: Visual representation of coded factors for Design of Experiment

3.1.4 Specimen Series

Specimens used are shown below in Figure 6 plotted onto the 1000°C isothermal section of iron, chromium, carbon ternary phase diagram, which was prepared for the Osaka project, a past UQMP research project. Inherently the steels are not shown as they are not on the phase diagram.

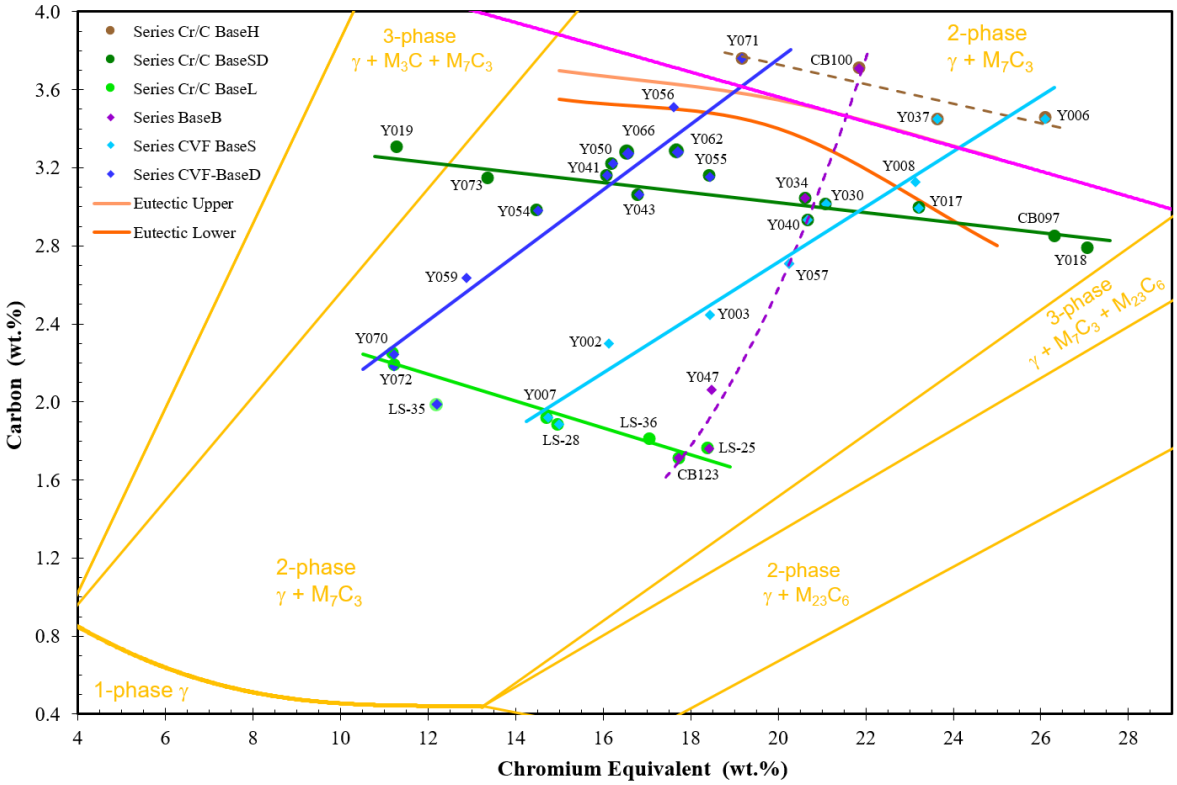

Figure 6: 1000°C isothermal section of Fe-Cr-C phase diagram, adapted from (Gates, et al., 2017)

The phase diagram was then used to separate the samples into three series of systematically varied CVF where Cr:C was held approximately constant and also into two series of systematically varied Cr:C where CVF was held approximately constant. These series are show below in Table 4.

Table 4: Series Designation

Cr:C Series		Cr-CVF Series		
Cr:C 1 Low CVF	**Cr:C 2 High CVF**	**Cr – CVF 1 (low Cr:C)**	**Cr – CVF 2 (Medium Cr:C)**	**Cr – CVF 3 (High Cr:C)**
CB123	Y073	CB100	LS-35	CB097
LS-25	CB097	Y041	Y002	CB123
LS-28	Y008	Y042,43,82,83,86	Y003	LS-25
LS-35	Y017	Y050	Y006	LS-36
LS-36	Y018	Y054	Y007	Y018
Y002	Y030	Y055	Y008	Y047
Y003	Y034	Y056	Y017	
Y007	Y038,57,65,74	Y059	Y030	
Y047	Y040	Y062	Y034	
Y059	Y041	Y066	Y037	
Y070	Y042,43,82,83,86	Y070	Y038,57,65,74	
Y072	Y050	Y071	Y040	
	Y054	Y072		
	Y055			
	Y062			
	Y066			

For the series outlined above, the related alloy parameter ranges are show below in Table 5.

Table 5: Alloy Parameter Ranges for Testing Series

Series	**Constant**		**Variable**	
Series Cr:C 1	CVF	14.6 to 25.2 vol%	Cr:C	4.9 to 10.8
Series Cr:C 2	CVF	28.2 to 36.1 vol%	Cr:C	17.9 to 42.6
Series Cr-CVF 1	Cr:C	4.9 to 5.9	CVF	17.9 to 42.6 vol%
Series Cr-CVF 2	Cr:C	6.8 to 7.9	CVF	14.6 to 41.8 vol%
Series Cr-CVF 3	Cr:C	9.2 to 10.8	CVF	15.6 to 34.4 vol%

3.2 Sample Set

This project is explicitly focusing on the effect of alloy parameters of CVF and Cr:C along with some steel samples to compare the performance of white cast irons with. The full list of specimens with their compositions used in testing can be found in Appendix B. In total there

were 40 different specimen types, 34 white cast irons and 6 steels with on average 5 blocks each, totalling 191 blocks.

3.3 Methodology of Preparation

3.3.1 Abrasive crushing and screening

The as-purchased rock had average particle size about 20mm, which is too coarse for the laboratory BMAT. Very coarse particles might not be able to the crushed in the laboratory mill, resulting in rounded pebbles circulating in the mill, which changes the conditions compared to normal ball mill conditions where the abrasive particles are continually fracturing to generate fresh sharp cutting edges. Standardly, the as-received abrasive needs to be crushed to less than 6.7mm particle sizes, which are able to be reliably broken in the ball mill. However testing will also explore particle sizes above this limit.

The Julius Kruttschnitt Mineral Research Centre (JKMRC) pilot plant was used for the crushing and screening of rocks for use as abrasives in BMAT testing.

Initial pre-start safety checks were completed and signed off upon inspecting the equipment for faults. Dust extraction was ensured to be switched on.

Crushing of rocks was done with a jaw crusher, the jaw adjusted to have a minimum opening of 7.0mm, selected by running a wad of aluminium foil through the crusher and narrowest point of the ball measured with callipers. A small bucket of as-received rock was initially poured into the hopper of the jaw crusher, the products were then screened with the Gilson screen shaker with 13.2mm, 9.5mm, 5.6mm and 1.7mm screens inserted. Weight percentages in each particle size distribution were calculated and if acceptable crushing and screening continued. Acceptable was considered to be when useful particle size ranges were maximised and waste (-1.7mm) and oversized particle size were minimised. The crushed abrasives were then bagged

at approximately 20kg each. This was repeated for each rock type of granite, quartzite, and basalt over the course of 8 sessions at JKMRC.

3.3.2 Heat Treatment and Preparation of ARNE and BK245 specimens

In addition to the existing set of white cast irons alloy samples, it was desired to enhance the specimen set with a more complete set of high-carbon martensitic steels to act as performance benchmark comparisons. The commercial steel alloys Uddeholm ARNE and Bohler K245 were available to be made into specimens, but needed to be heat treated to provide the required high-hardness, lightly tempered martensite microstructure.

The high temperature furnace was preheated to 850^{o}C, all 18 block specimens (9 of each alloy) were labelled then placed in an open topped box. The box was layered with coke followed by sand with the specimens finally another layer of coke. The basket was placed into the furnace and a Type K thermocouple was inserted through top of the furnace, so that its tip was in contact with surface of the middle sample, connected to a Center 309 data logger thermometer. Samples were heated until surface temperature reached an austenitizing temperature of 840^{o}C then held above this temperature for 60 minutes. Temperature was manually adjusted on the furnace to hold the surface temperature at 850^{o}C. Once the time had elapsed, the samples were removed from the furnace and tipped into a wire mesh basket to discard the coke and sand. This basket was then submerged in an oil tank to oil quench the specimens.

After hardening by austenitizing and quenching, the alloys were tempered to recover sufficient fracture toughness. For the Bohler K245, three specimens were tempered at these temperatures respectively: 140, 200, 260^{o}C using the same method of timing and furnace temperature selection as the austenitization. Then held for two hours at the selected surface temperature then air cooled. With respect to the ARNE samples, five specimens treated at 200^{o}C and four at 260^{o}C with these placed in the furnace concurrently with K245, held for two hours and air cooled.

Bohler K245 and Uddeholm ARNE specimens had the edges and vertices of the samples rounded with the linisher to avoid chipping of the samples while in the ball mill.

3.3.3 Vickers Hardness Testing

For hardness testing, a specimen of each alloy and each heat treatment was ground and polished on Struers TegraPol-31 sample preparation machines using SiC sand paper with the following grits in respective order 320, 600 then 1200, held at each level till damage from previous level was non visible.

Using Vickers hardness machines with a force of 30kgf and 12 second dwell time. 10 measurements were taken per block in a cross pattern across plus a single random point, this was done attempting to hold the normalised standard deviation below 3%.

3.3.3 Surface Grinding

Of the selected alloys, as they had be previously used in other testing, surface quality was quite poor on some of the selected specimens. Consequently, these specimens had to be surface ground to smooth out the surfaces done with low porosity grinding segments.

4.0 Results

4.1 Evaluation of Results

Weights taken at prior to testing then at the end of each test, done consecutively, where the post weight of the test becomes the pre weight for the following test. Slight adjustments were made if the blocked had to be relabelled or edges rounded again to remove damage from chips. Weighing was done on a Mettler Toledo precision scale.

4.1.1 Calculations

Weight loss has been calculated using:

$$Nomalized\ weight\ loss\left(\frac{mg}{100g}\right) = \frac{(pre\ weight(mg)) - (post\ weight(mg))}{100 * pre\ weight}$$

Values of error shown are Standard Error calculated by:

$$\frac{\sigma}{\sqrt{n-1}}$$

Where σ is the Standard Deviation of the data for the specific alloy in that given test, and n is the number of specimens of the specific alloy.

Benefit ratio

$$BR = \frac{Average\ weight\ loss\ of\ Steels}{Average\ weight\ loss\ of\ White\ Cast\ Irons}$$

For reference materials, surface area of the block specimens is found by taking the average of two measurements for length, three for width and height, then calculated as a rectangular prism.

Trend lines for the alloy parameter graphs are all 2nd order polynomial estimations

4.2 Testing Condition

To provide an overview of the effects of the testing conditions, Figure 7 shows the benefit ratio as calculated in 4.1.1 (which compares weight lost by the average steel to weight loss by the average white cast iron), as a function of abrasive type, abrasive feed particle size and test duration. A higher benefit ratio implies the greater performance.

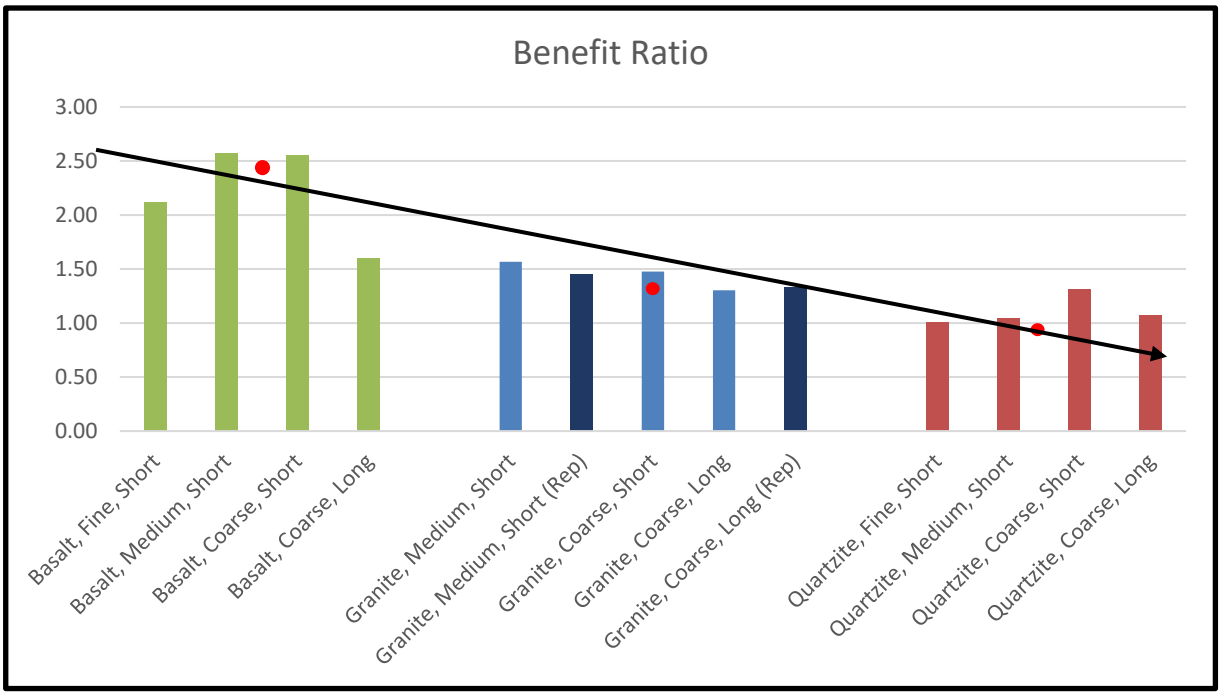

Figure 7: Benefit ratio of White Cast Irons over Steels in varying testing conditions

Firstly considering the effect of abrasive type, which are shown in Figure 7 in increasing order of increasing expected hardness (or competence) of the abrasive rock type. The benefit of white cast irons is shown to decrease with increasing hardness of rock. In the quartzite, the benefit is even lost completely, with the white cast iron giving only equal performance to the steels in three of the four tests.

Secondly the effect of feed particle size distribution. Increasing feed particle size was shown to improve the performance of white cast irons over steel, trending upward in basalt and quartzite abrasive types, but level within statistical scatter for granite.

Finally, increasing test duration was noted to decrease the benefit of white cast irons over steels given the same starting conditions in all abrasive types.

4.3 Alloy Parameters

In this section, wear rates (mg/100g) are plotted against CVF (percentage of volume) and Cr:C (weight percent chromium to weight percent carbon) for each testing condition respectively. Unlike in 4.2 Testing Condition, the where benefit ratio was shown, the charts are all the absolute values of wear rate as calculated in 4.1.1 A higher wear rate means poorer performance. Further, all graphs use the wear rate so they can be compared with each other allowing observations of the effect of test conditions. The headings of the following subsections represent the testing conditions as defined in 3.1.1

4.3.1.1 Basalt, Fine, Short

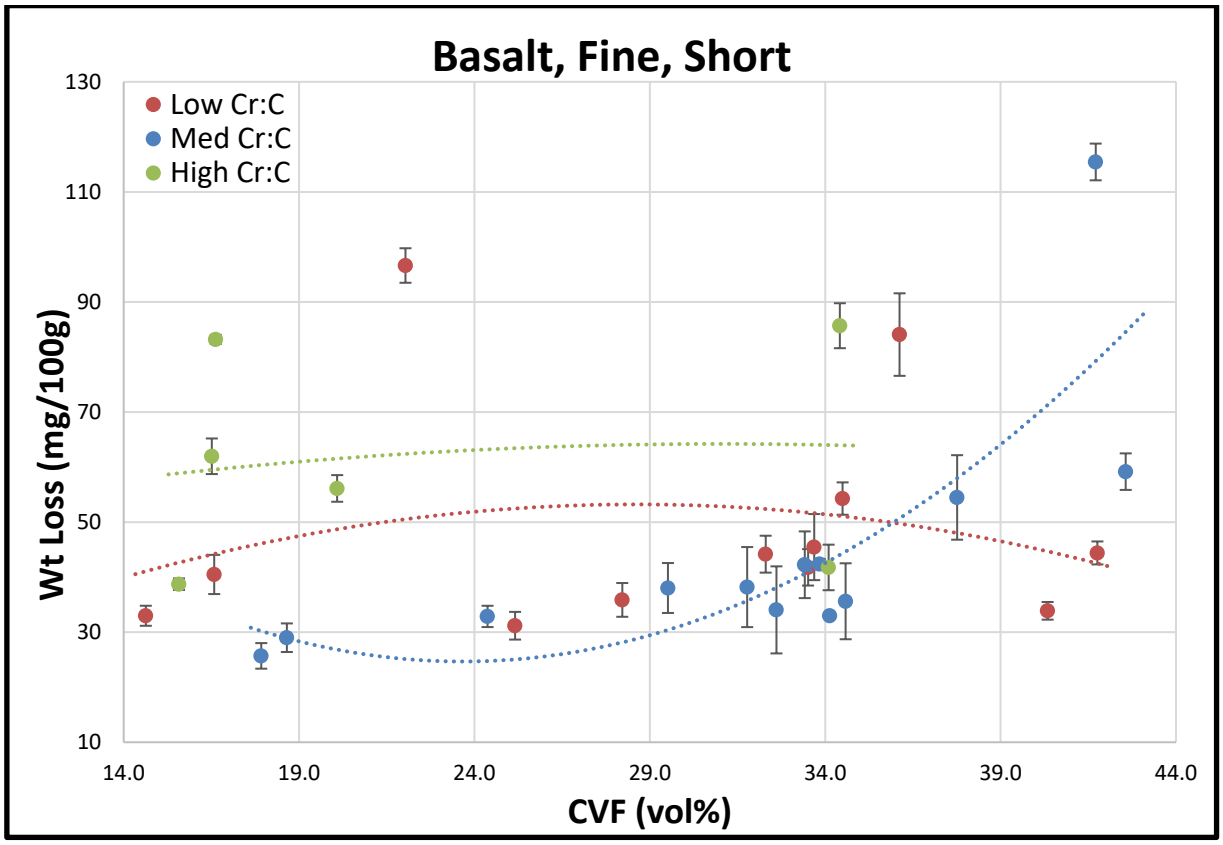

Figure 8: Effect of CVF in Basalt, Fine, Short

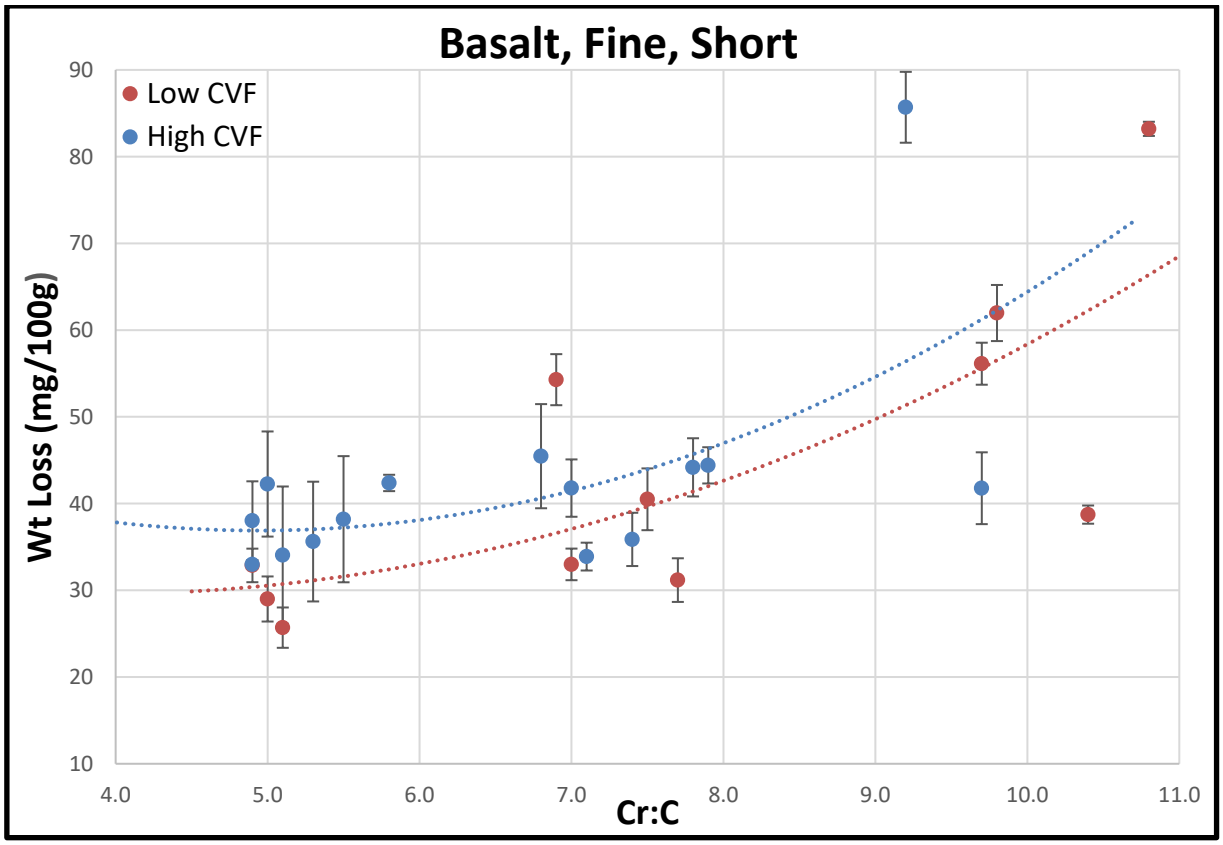

Figure 9: Effect of Cr:C in Basalt, Fine, Short

4.3.1.2 Basalt, Medium, Short

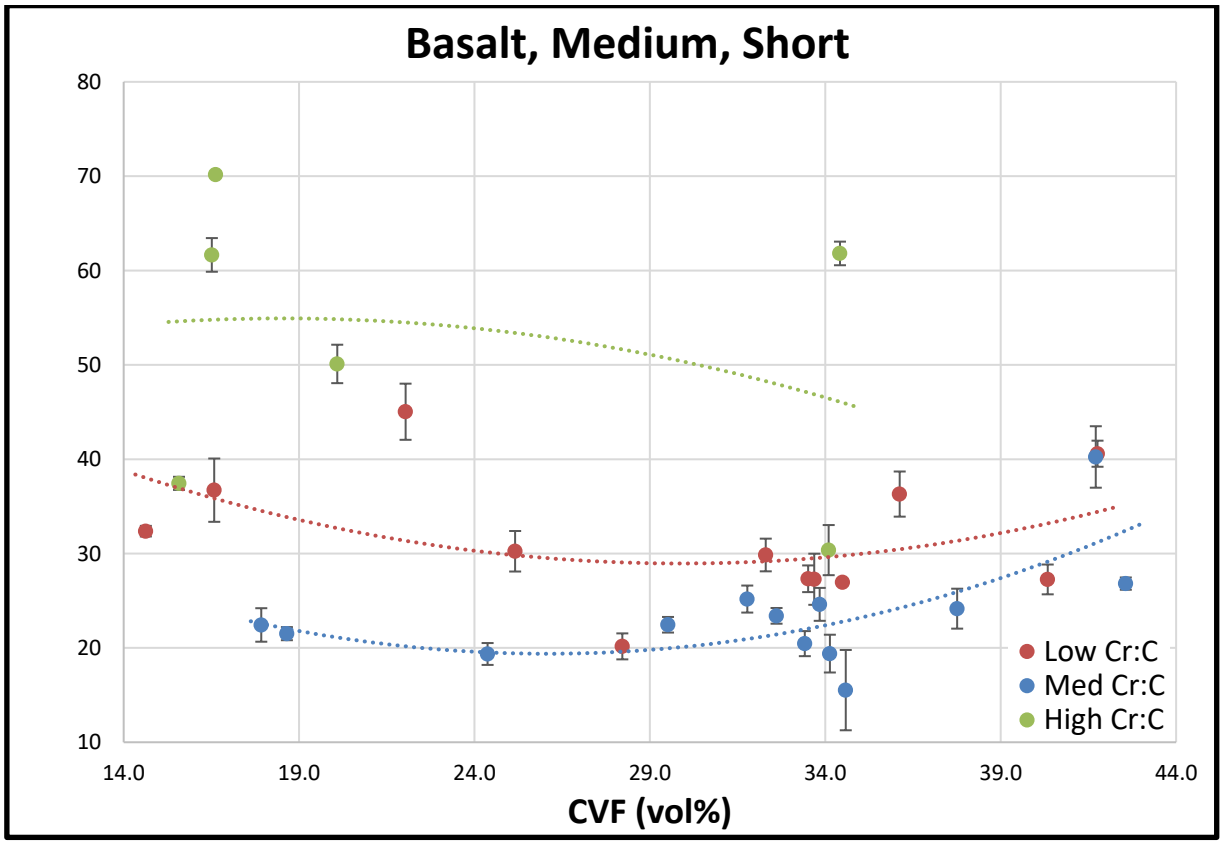

Figure 10: Effect of CVF in Basalt, Medium, Short

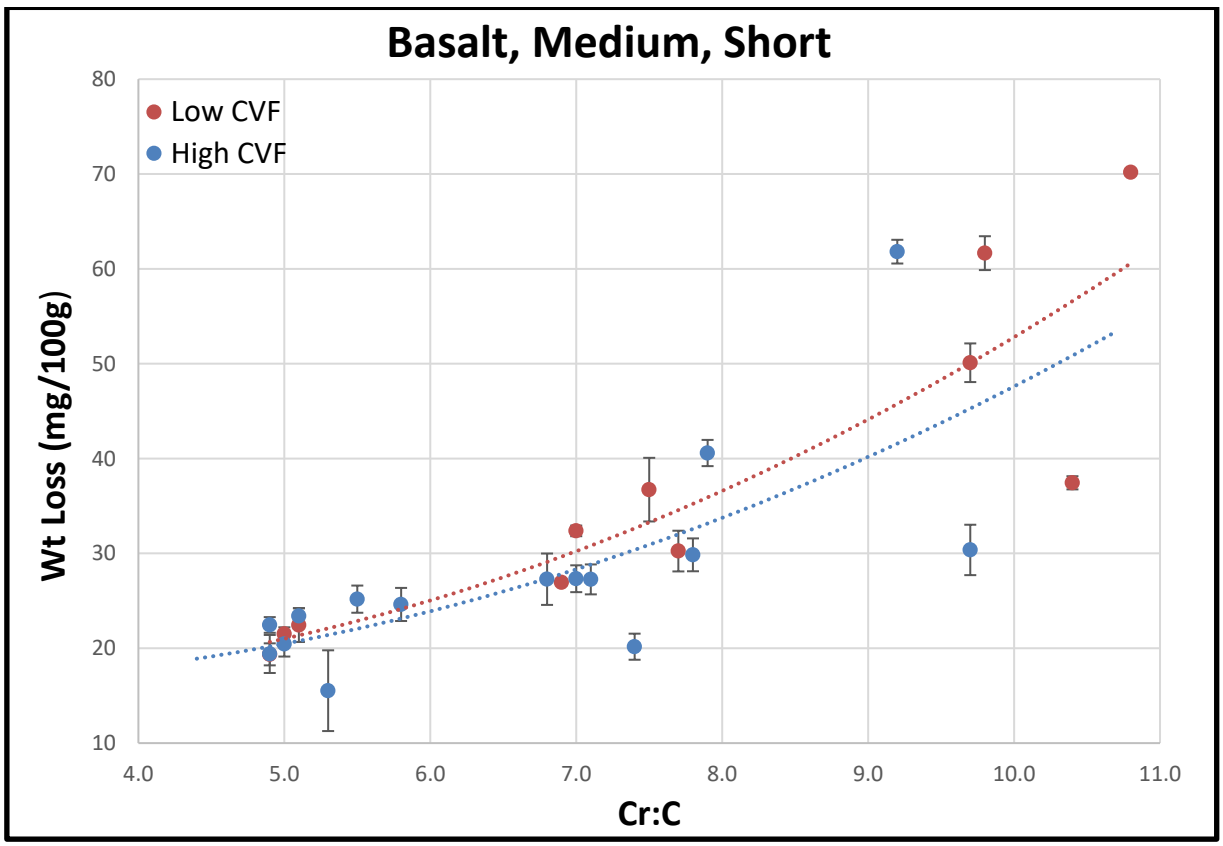

Figure 11: Effect of Cr:C in Basalt, Medium, Short

4.3.1.3 Basalt, Coarse, Short

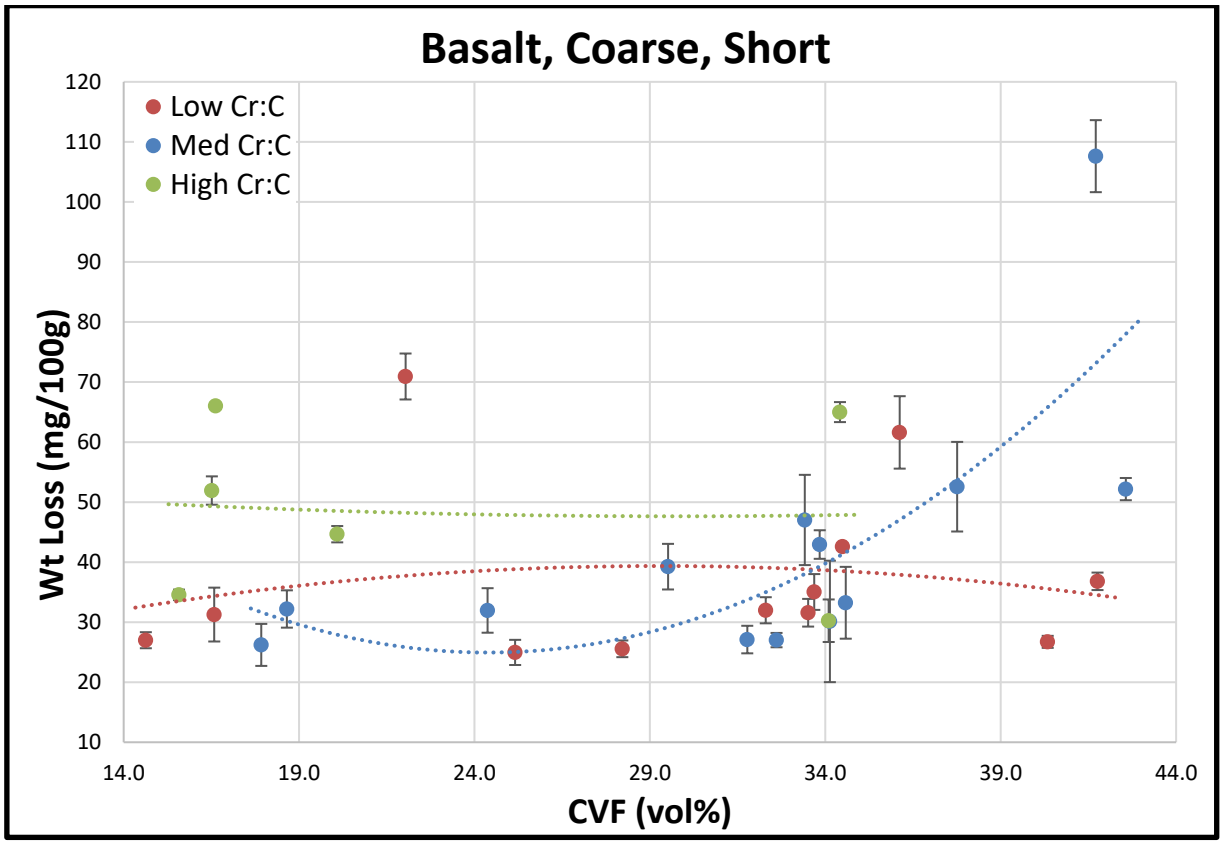

Figure 12: Effect of CVF in Basalt, Coarse, Short

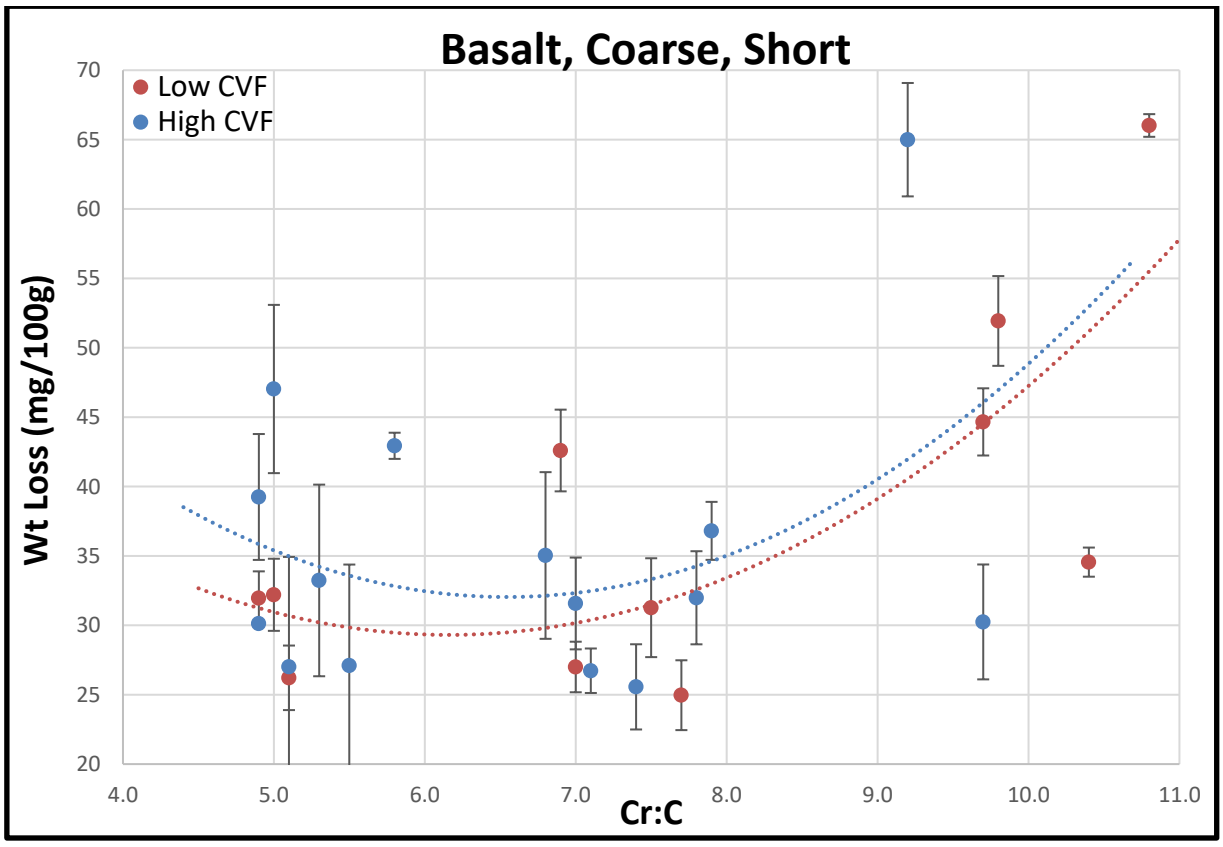

Figure 13: Effect of Cr:C in Basalt, Coarse, Short

4.3.1.4 Basalt, Coarse, Short Replicate

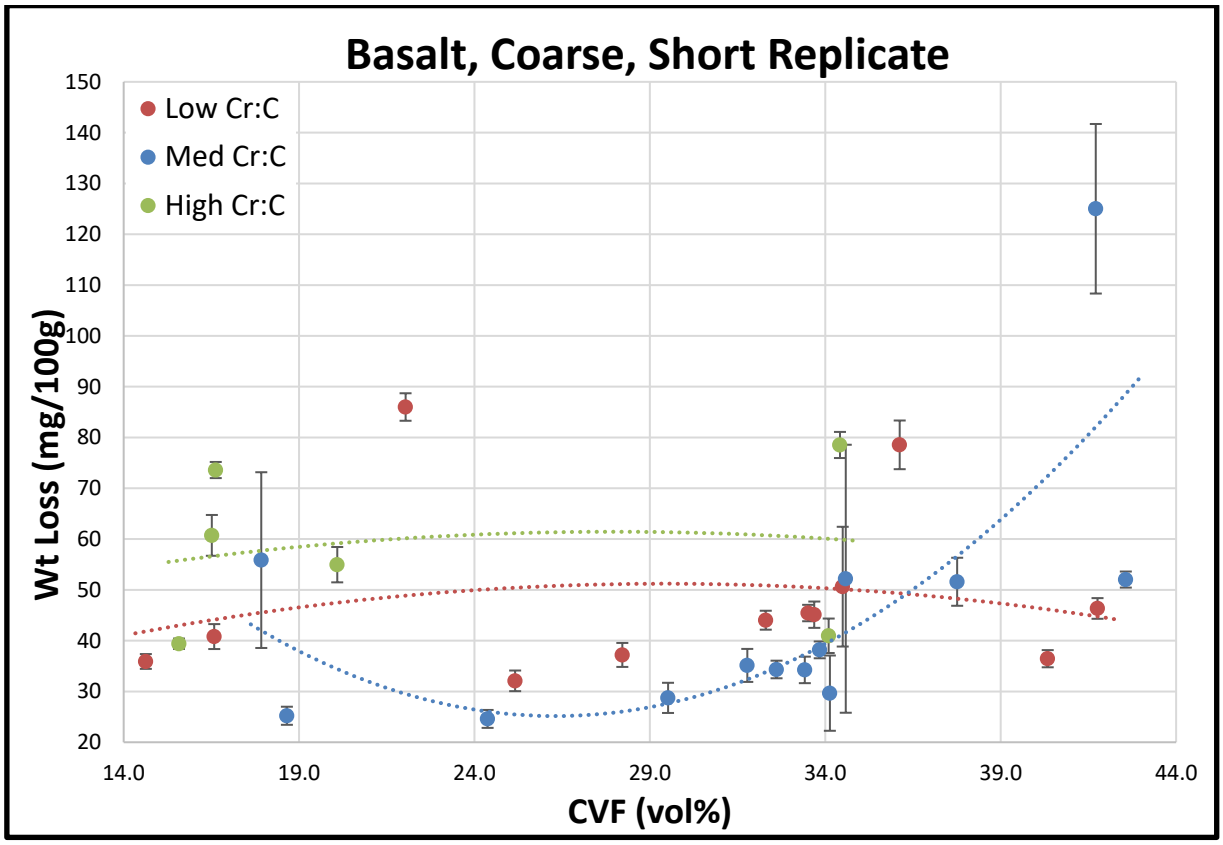

Figure 14: Effect of CVF in Basalt, Coarse, Short Replicate

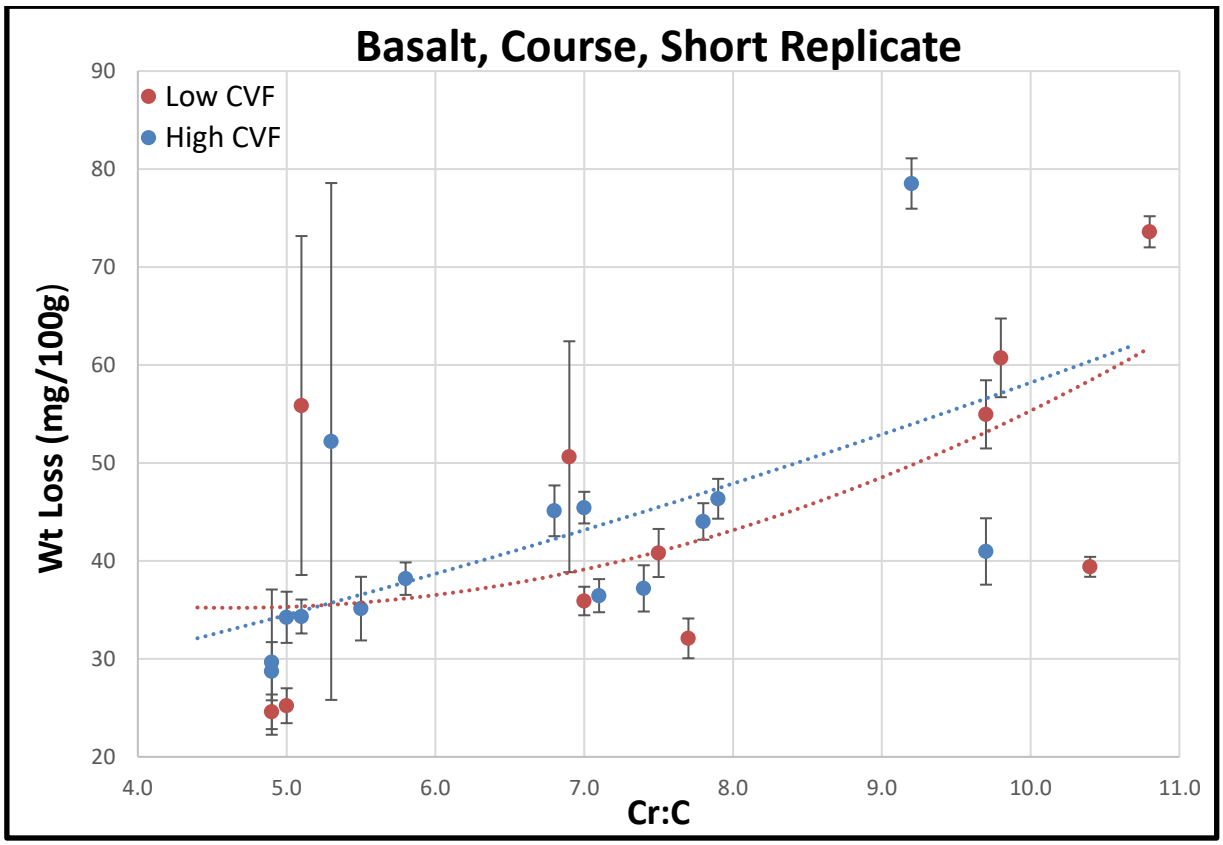

Figure 15: Effect of Cr:C in Basalt, Coarse, Short Replicate

4.3.1.5 Basalt, Coarse, Long

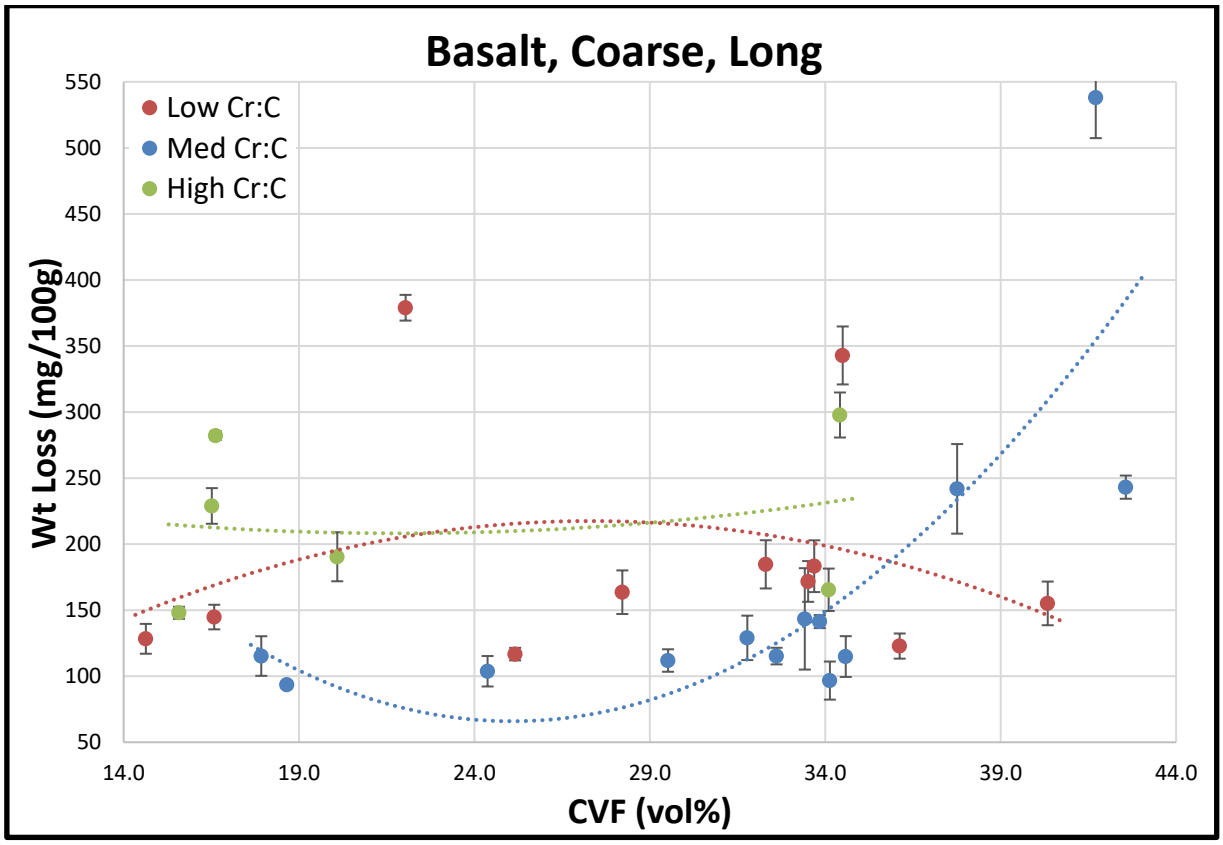

Figure 16: Effect of CVF in Basalt, Coarse, Long

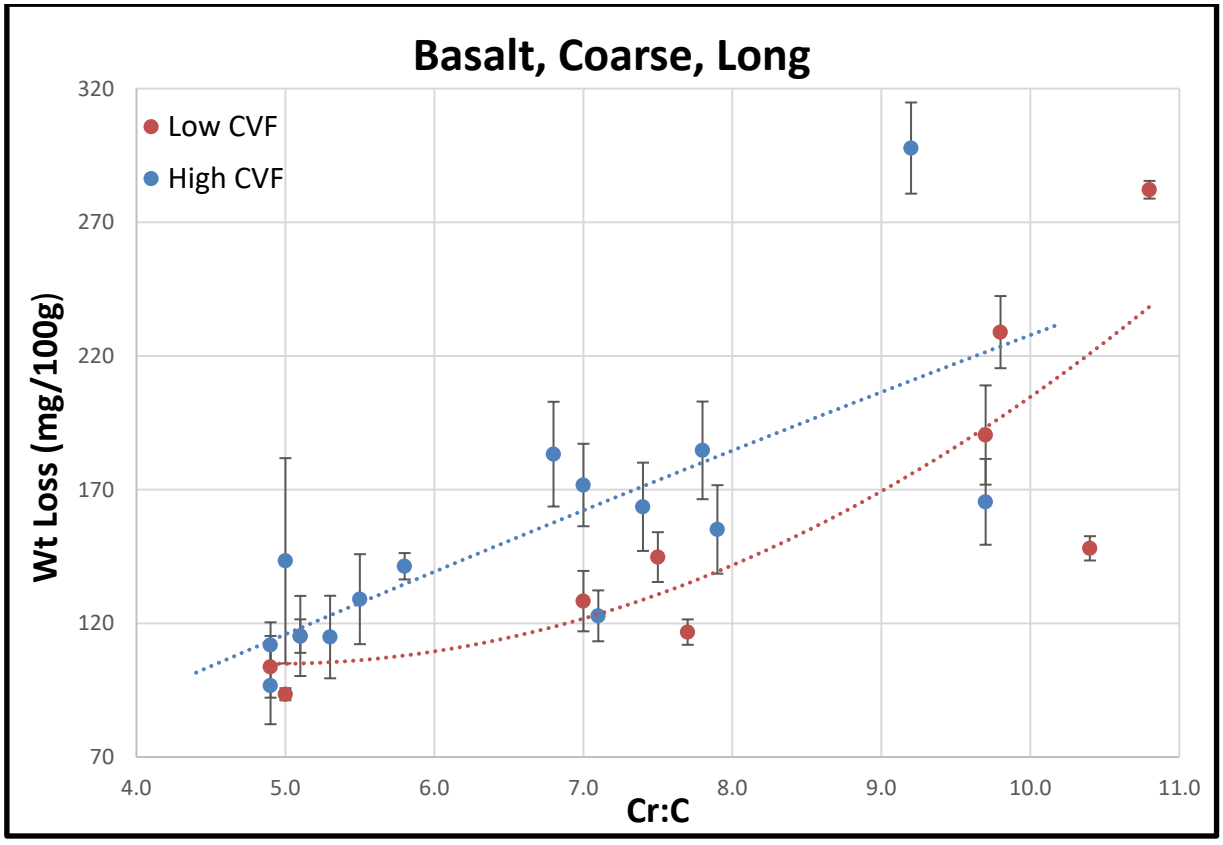

Figure 17: Effect of Cr:C in Basalt, Coarse, Long

4.3.1.6 Granite, Medium, Short

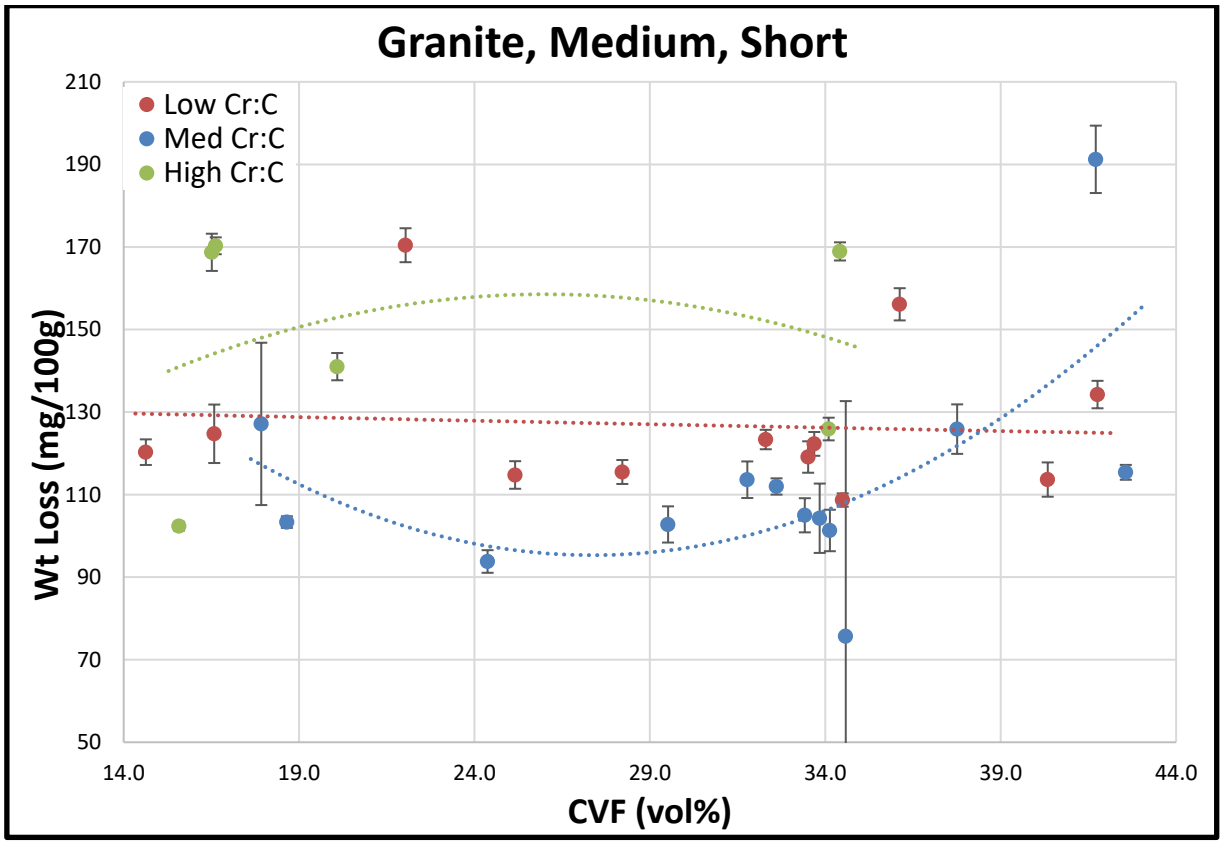

Figure 18: Effect of CVF in Granite, Medium, Short

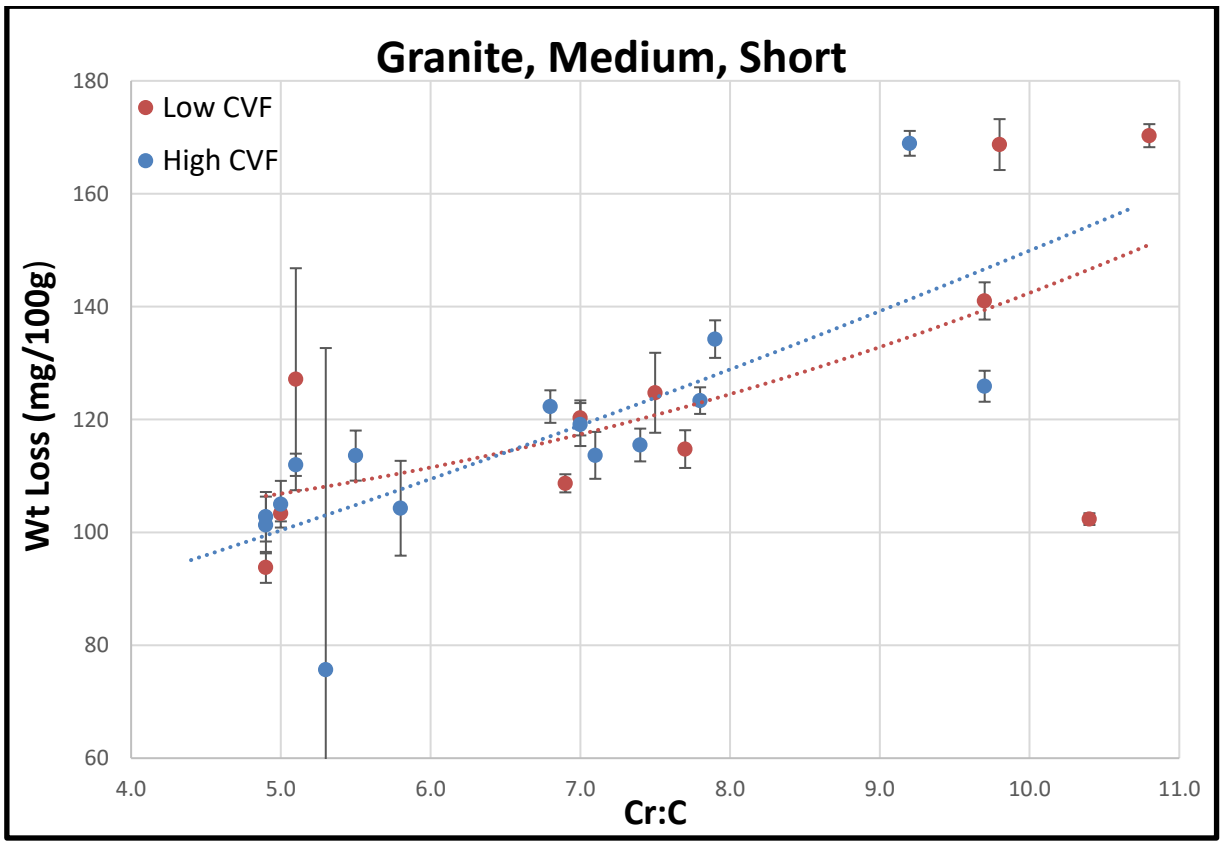

Figure 19: Effect of Cr:C in Granite, Medium, Short

4.3.1.7 Granite, Medium, Short Replicate

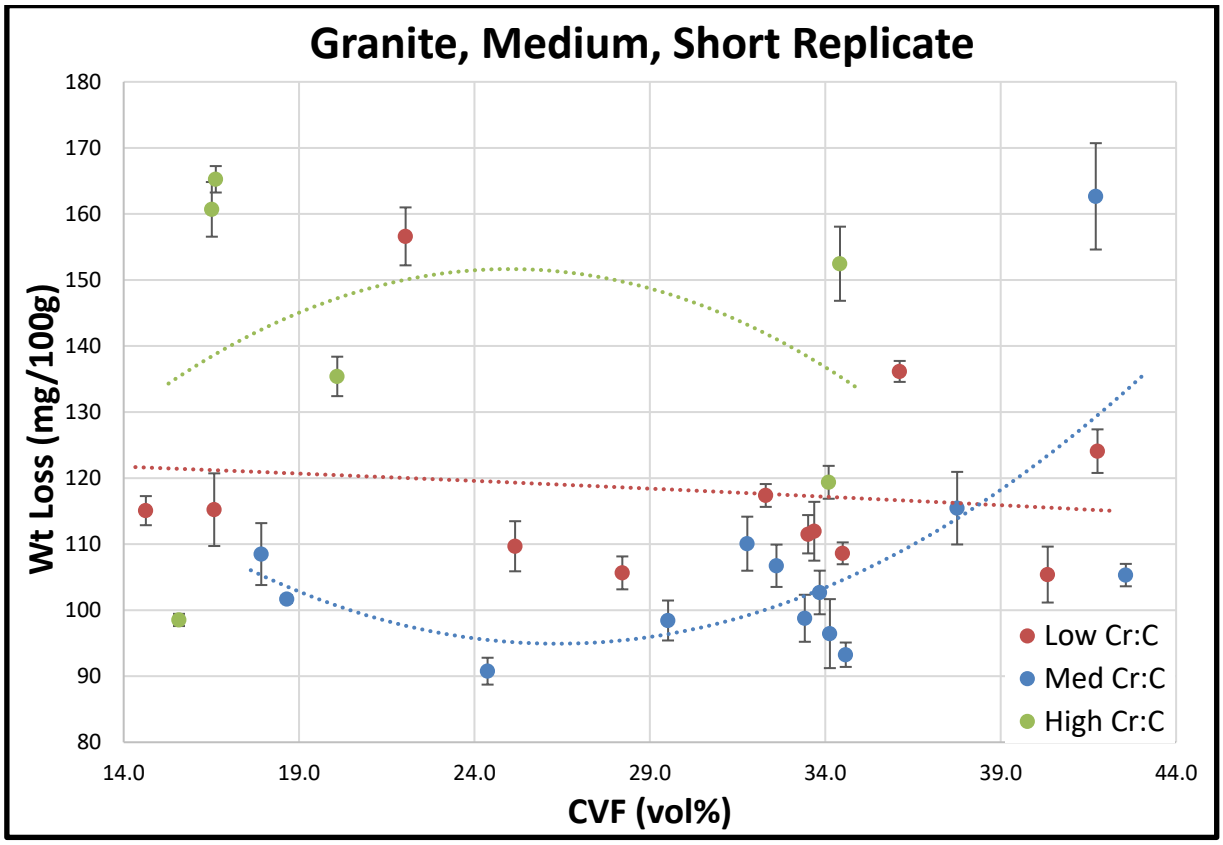

Figure 20: Effect of CVF in Granite, Medium, Short Replicate

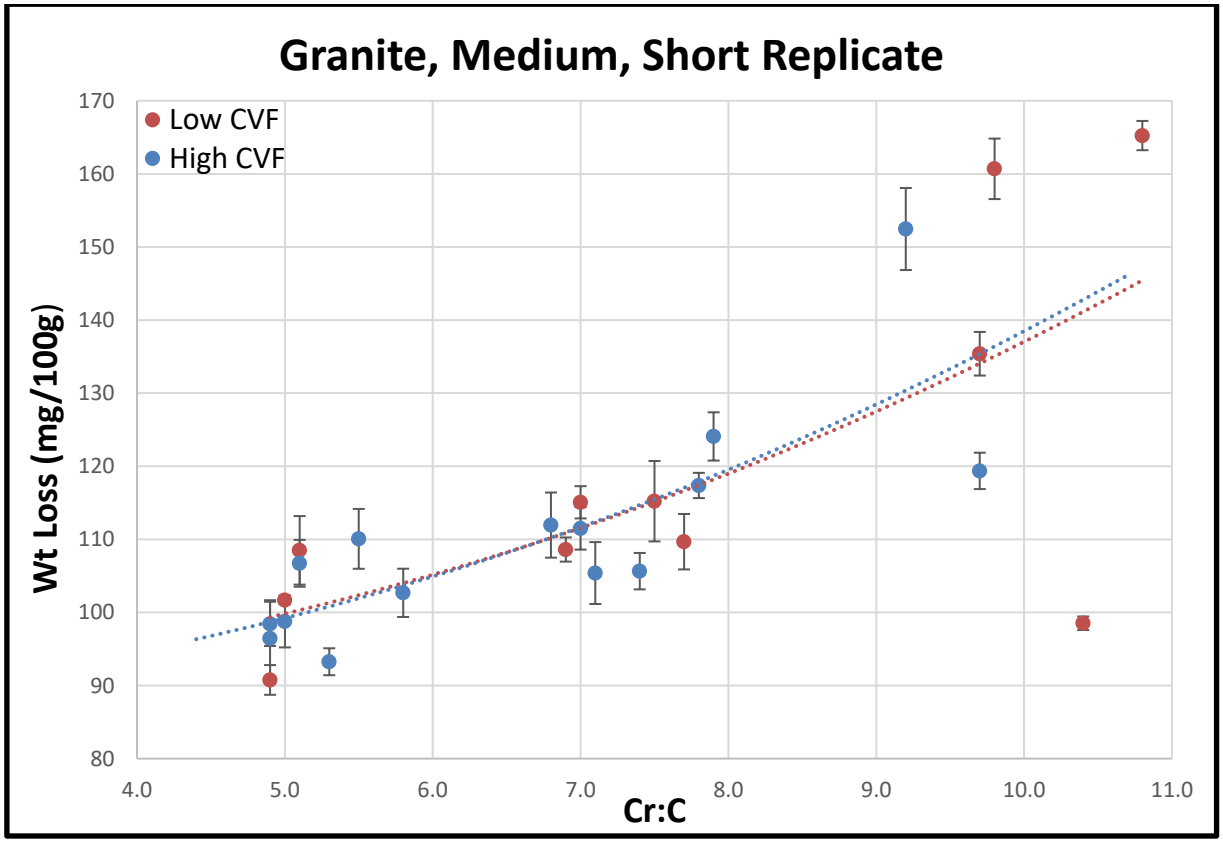

Figure 21: Effect of Cr:C in Granite, Medium, Short Replicate

4.3.1.8 Granite, Coarse, Short

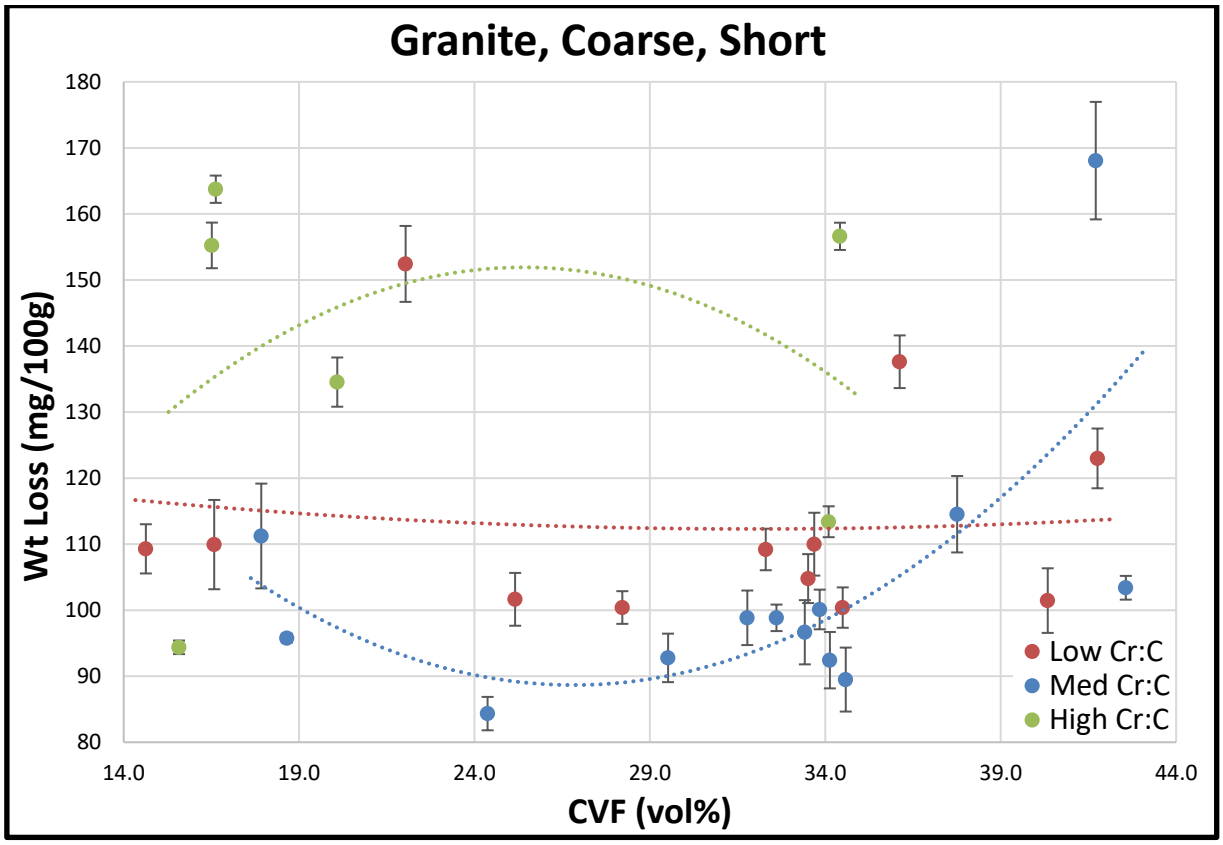

Figure 22: Effect of CVF in Granite, Coarse, Short

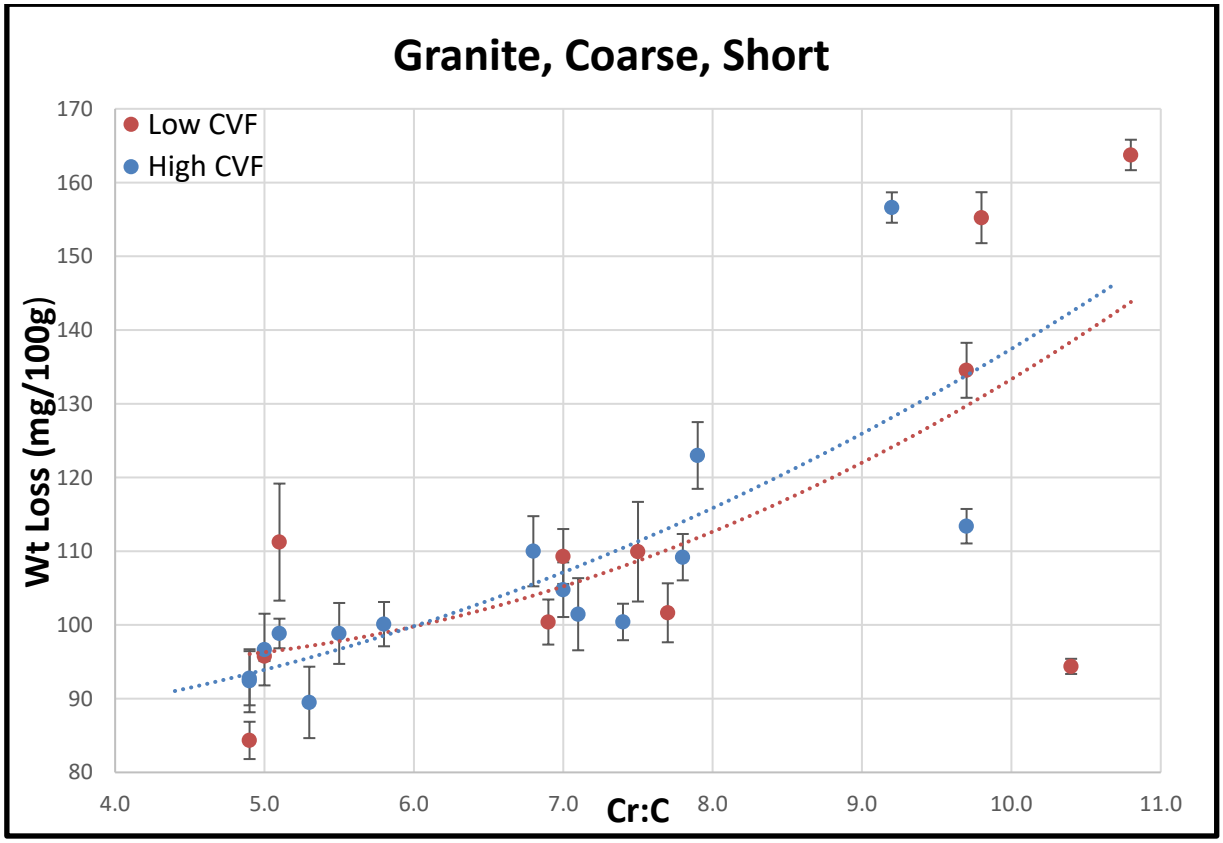

Figure 23: Effect of Cr:C in Granite, Coarse, Short

4.3.1.9 Granite, Coarse, Long

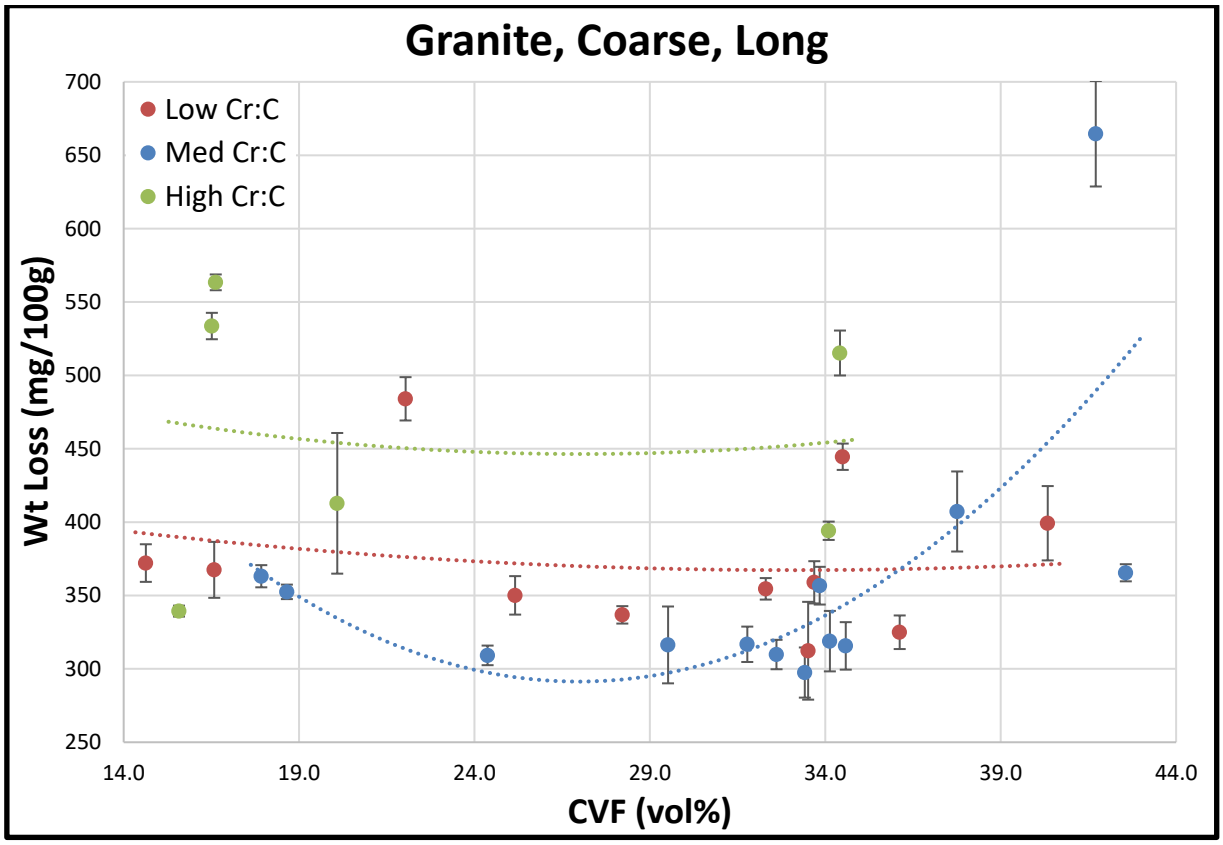

Figure 24: Effect of CVF in Granite, Coarse, Long

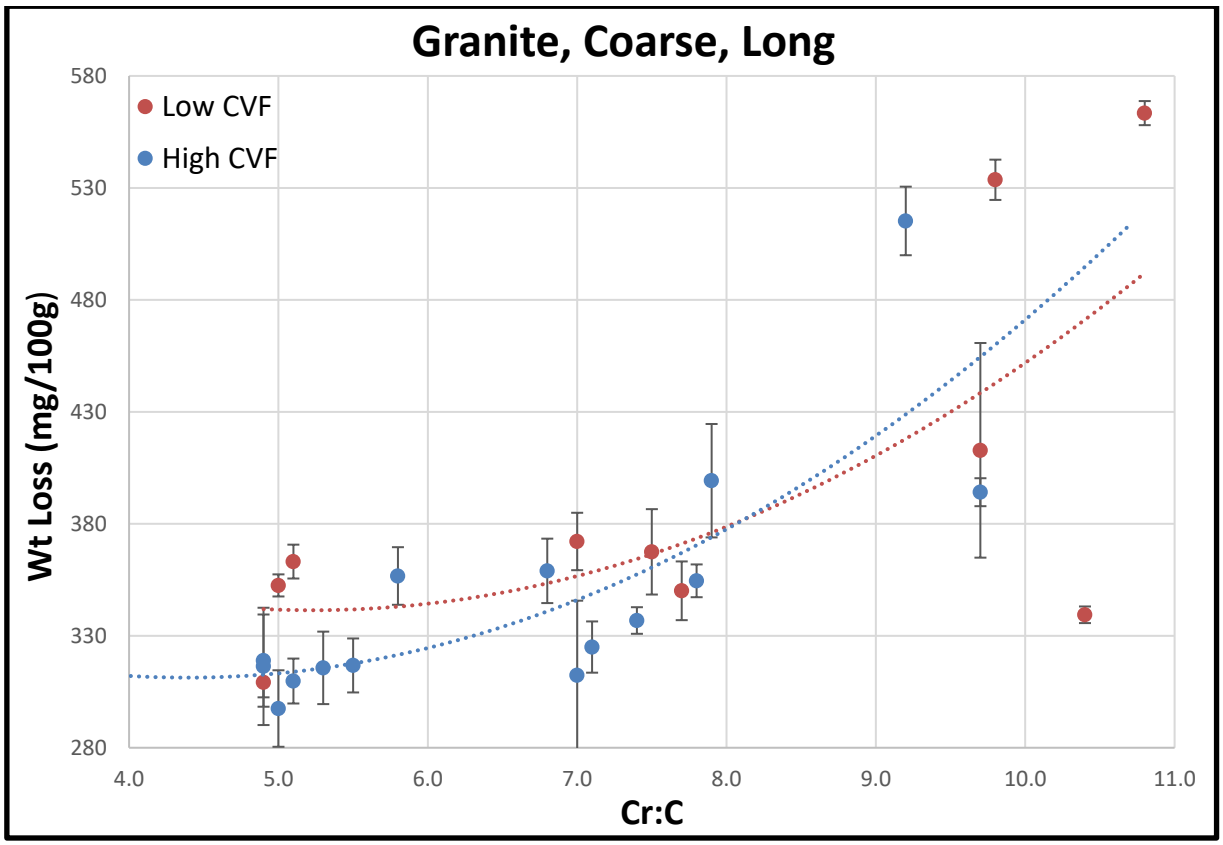

Figure 25: Effect of Cr:C in Granite, Coarse, Long

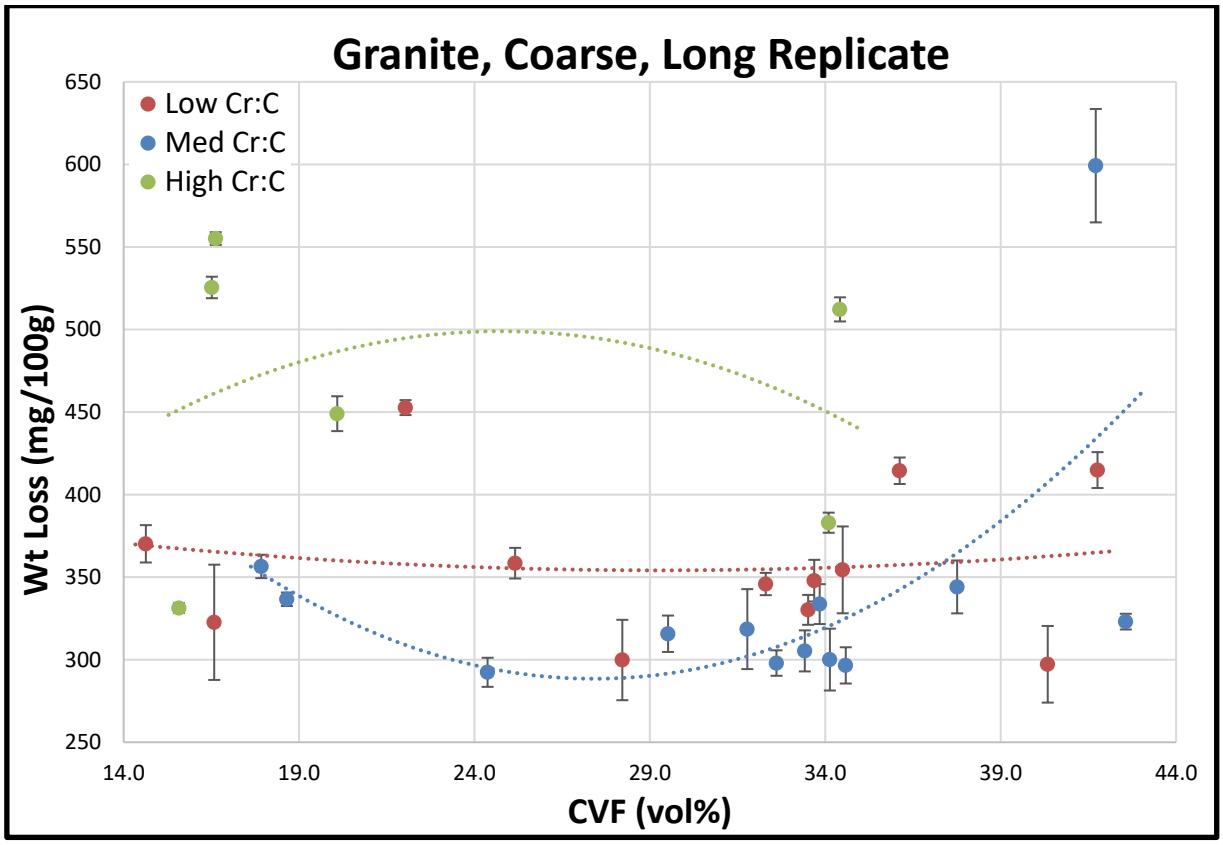

Figure 26: Effect of CVF in Granite, Coarse, Long Replicate

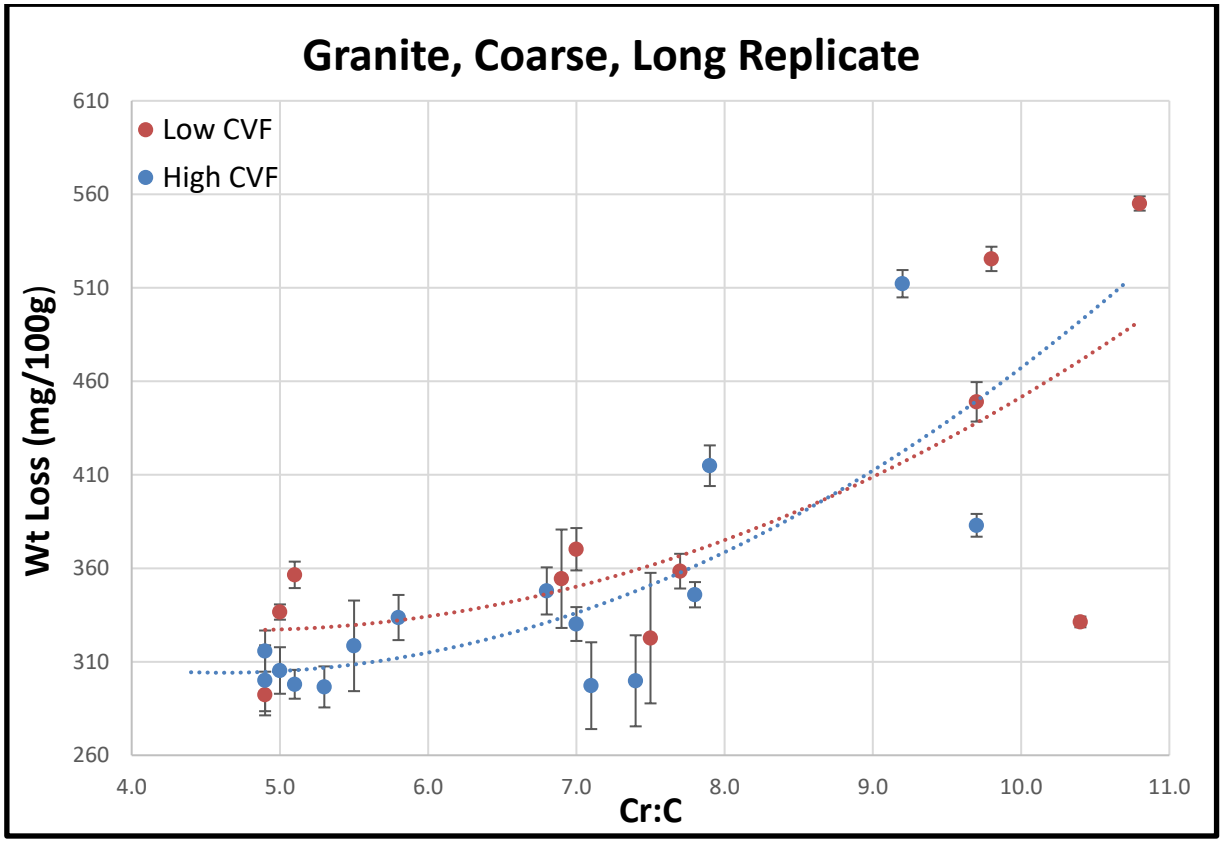

Figure 27: Effect of Cr:C in Granite, Coarse, Long Replicate

4.3.1.11 Quartzite, Fine, Short

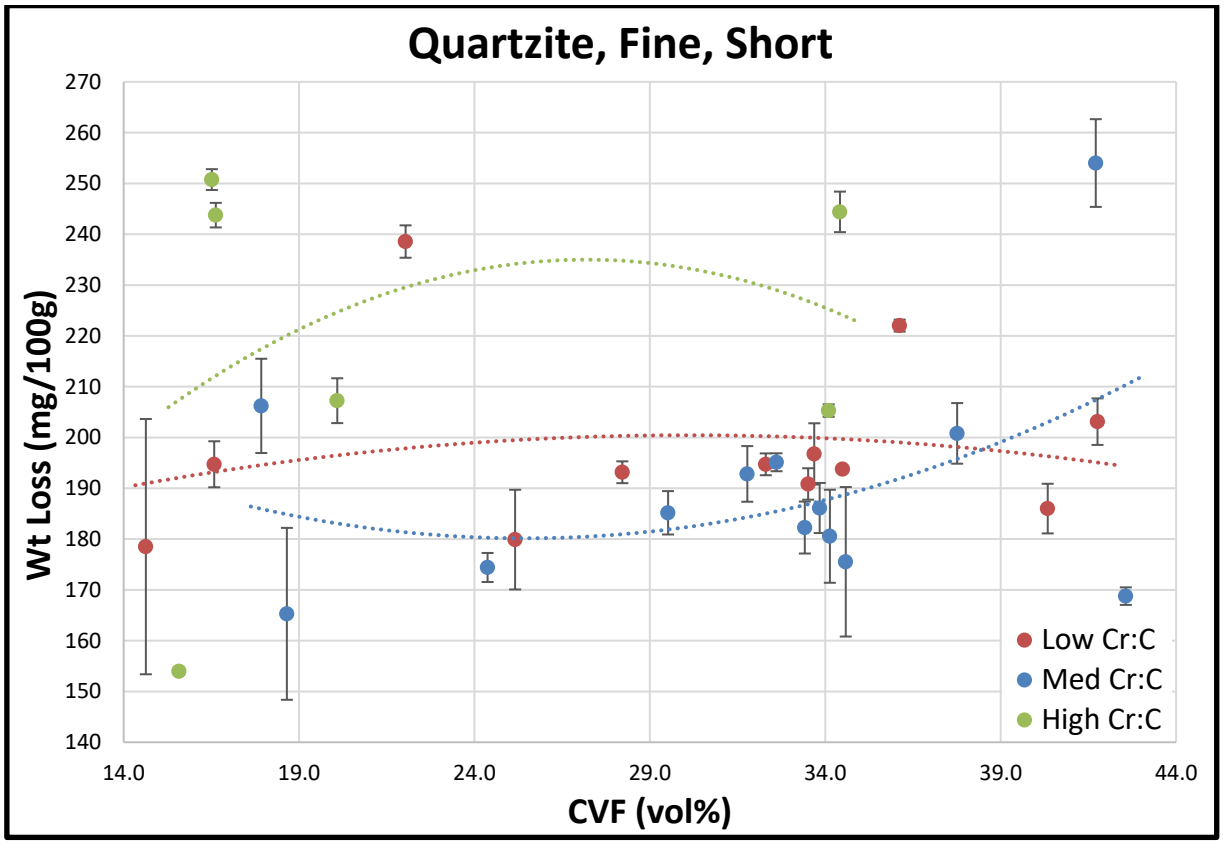

Figure 28: Effect of CVF in Quartzite, Fine, Short

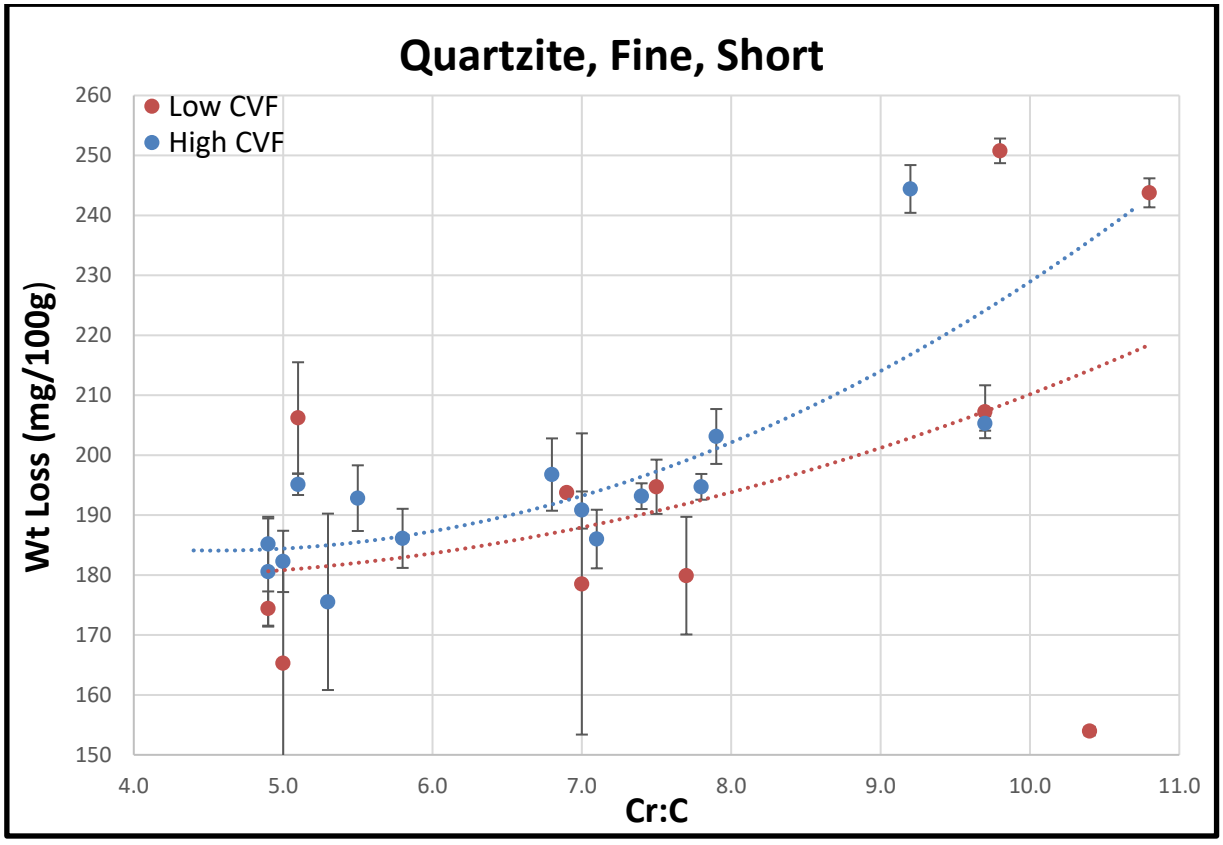

Figure 29: Effect of Cr:C in Quartzite, Fine, Short

4.3.1.12 Quartzite, Medium, Short

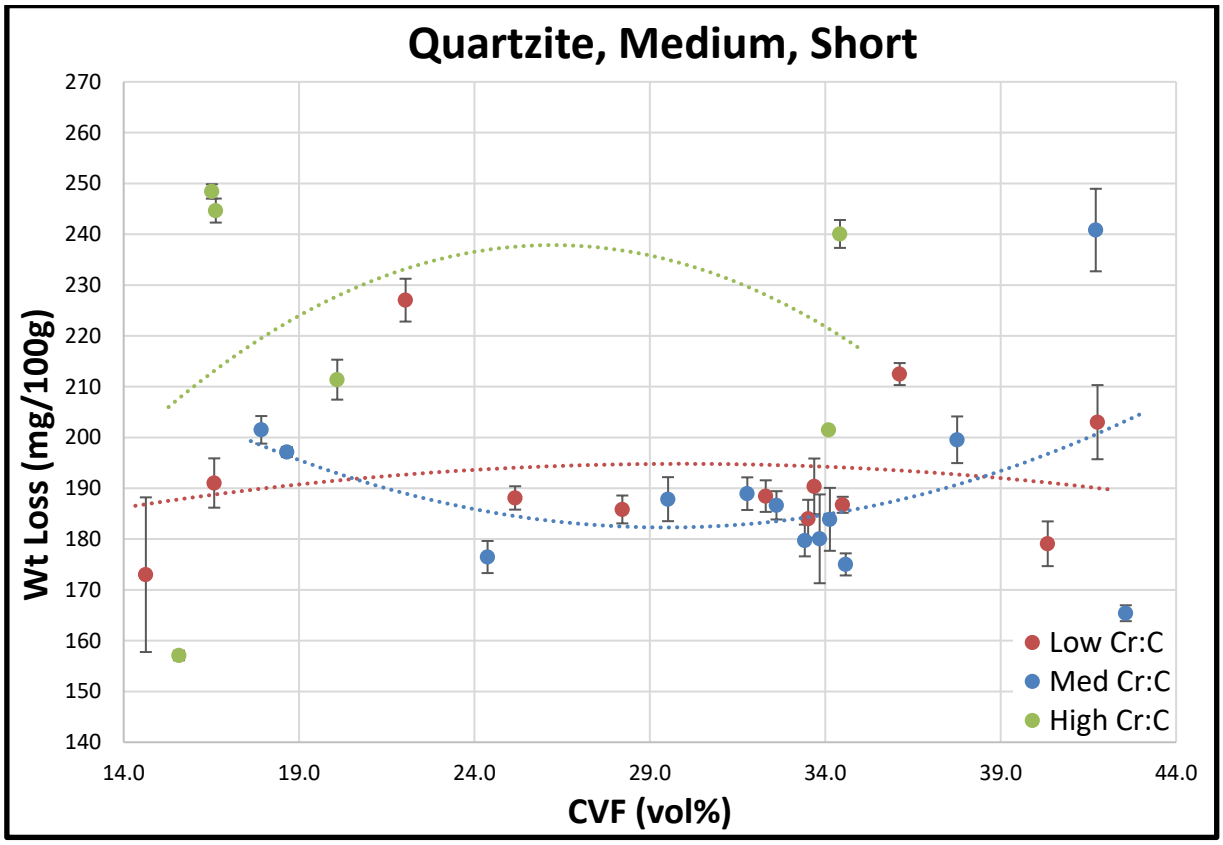

Figure 30: Effect of CVF in Quartzite, Medium, Short

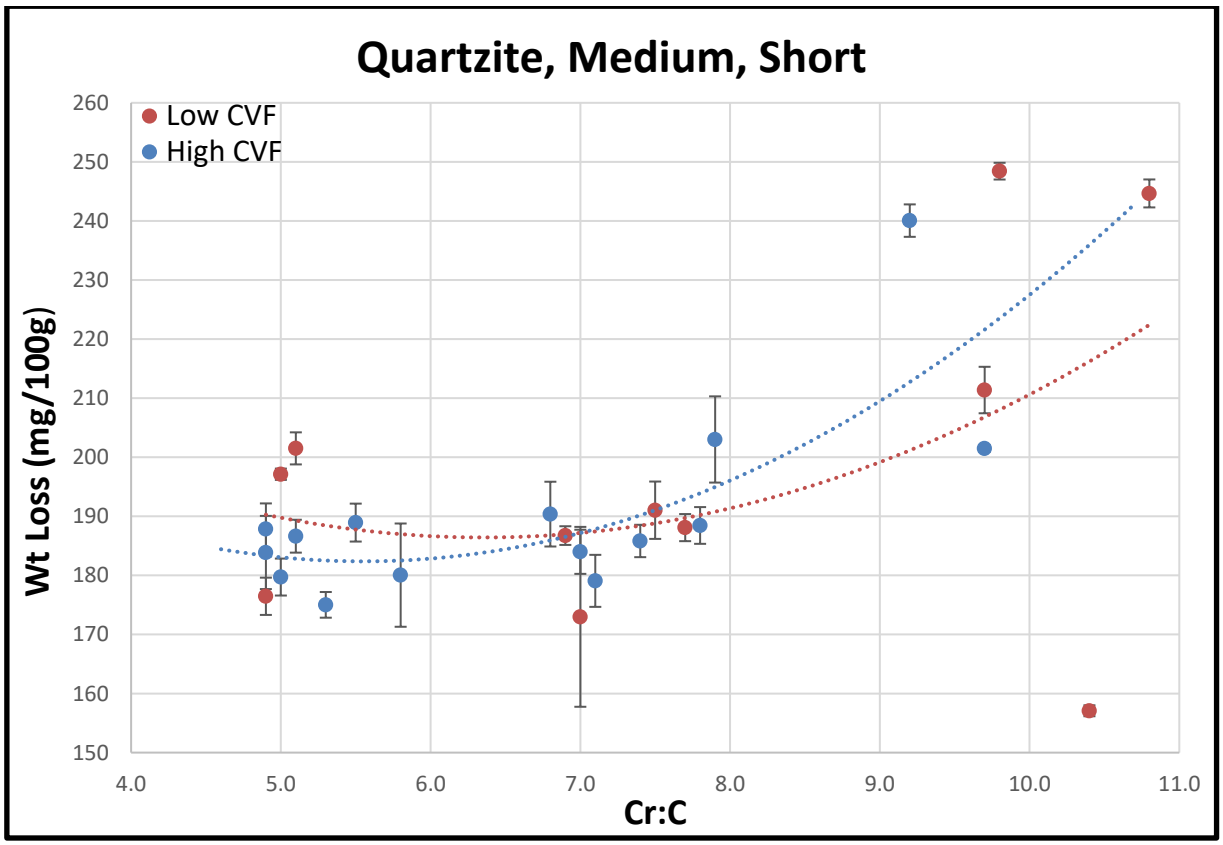

Figure 31: Effect of Cr:C in Quartzite, Medium, Short

4.3.1.13 Quartzite, Coarse, Short

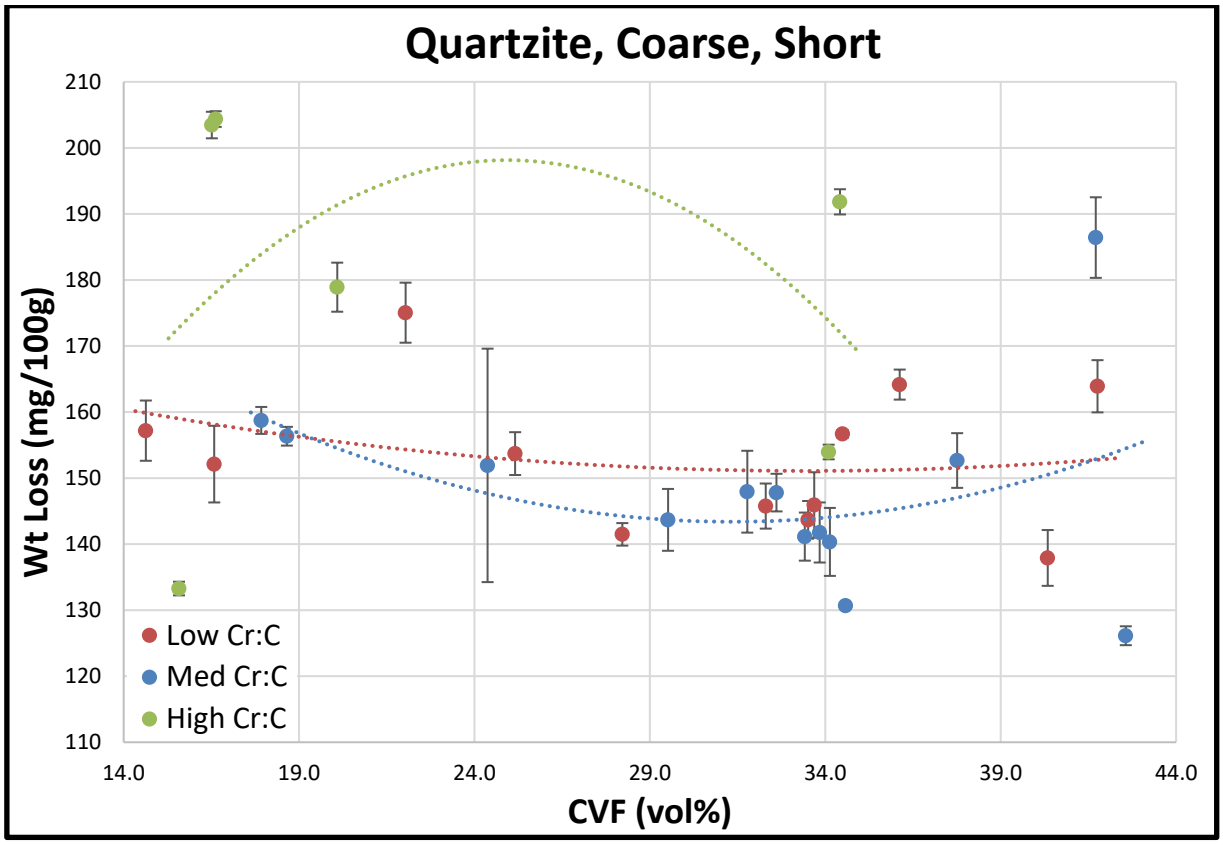

Figure 32: Effect of CVF in Quartzite, Coarse, Short

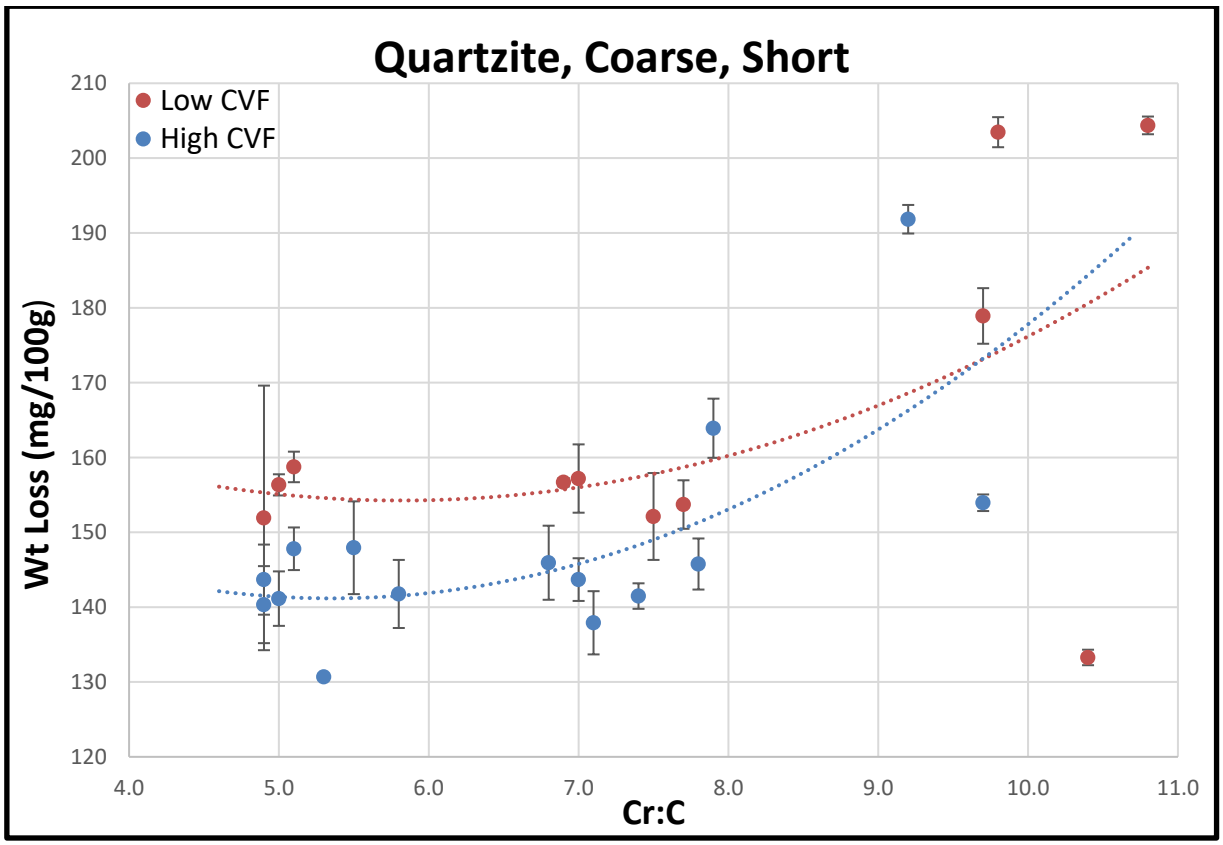

Figure 33: Effect of Cr:C in Quartzite, Coarse, Short

4.3.1.14 Quartzite, Coarse, Long

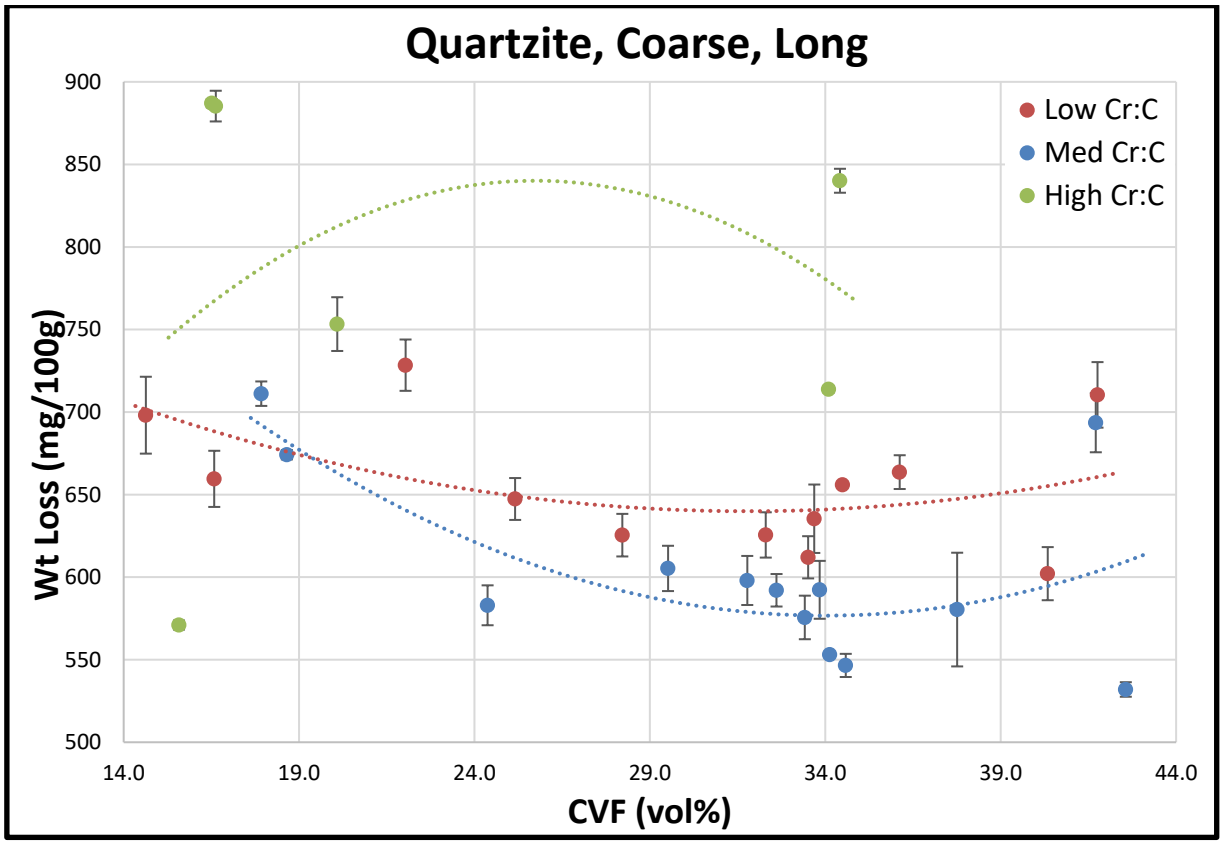

Figure 34: Effect of CVF in Quartzite, Coarse, Long

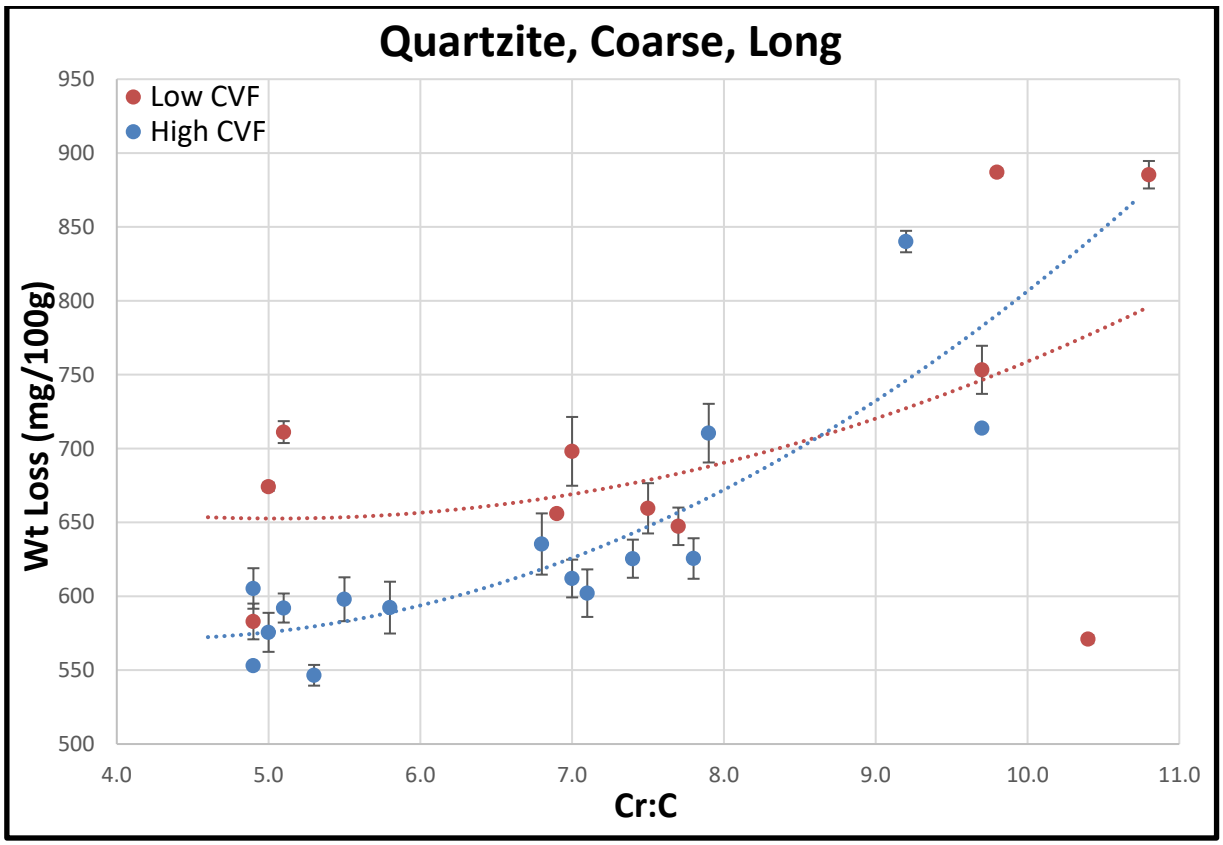

Figure 35: Effect of Cr:C in Quartzite, Coarse, Long

4.4 Alloy Performance Overall

Below in Table 6, the results for every alloy plotted in 4.3 in order of wear rate, averaged over all tests completed.

Table 6: Average Normalized Wear Rate over All Tests for All Plotted White Cast Irons

SPECIMEN LABEL	**AVERAGE NORMALIZED WEAR RATE OVER ALL TESTS (mg/100g)**
62_	153.56
59_	154.91
66_	155.42
50_	162.10
123_	162.82
41_	162.93
54_	163.46
40_	163.92
43_, 82_	167.15
35_	169.98
70_	170.30
8_	170.46
55_	170.51
30_	173.31
100_ (OR _XX)	174.16
7_	174.21
3_	180.82
17_	181.40
2_	182.17
34_	182.55
72_	184.97
56_	190.38
18_	194.22
57_	199.94
47_	215.71
37_	225.33
6_	247.35
36_	257.04
97_	257.90
25_	269.36
71_	291.93

Specimen Y062 (Cr/C055-BD) when averaged across all testing conditions, had the lowest average wear rate.

4.5 Hardness

The collected hardness data for the specimens used in testing is shown in Figure 36. Full data collection is shown in Appendix C: Hardness Data.

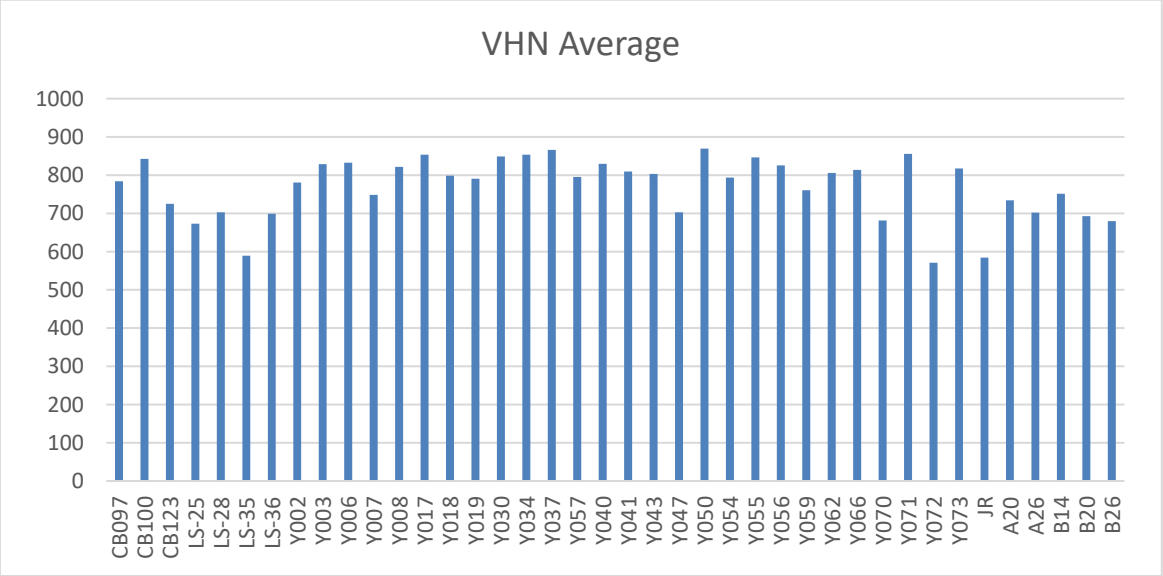

Figure 36: Vickers Hardness Data of Test Specimens

5.0 Discussion

5.1 Testing Conditions

The effects of testing condition did not show the benefit ratios expected prior to testing. The effect of abrasive type is logical whereby as competence of the abrasive increases, the ability for a particle to damage the carbide phase through fracture as the well as the abrasive wear of the matrix, meaning the tougher abrasives, performance of the steels and white cast irons was comparable, as they can wear both the matrix and fracture the carbide phase.

When considering feed size, it was initially thought that with larger abrasive particles, the benefit ratio over steels would be lower, as these larger particles are able to produce high stress abrasion which can damage the carbide phases. However the effect of feed size is observed to be that in smaller sizes the benefit of white cast irons over steels is less. This may be due to these fine particles being able to contact the relatively soft matrix, without being as easily interrupted by the carbides, allowing the matrix to be worn away, exposing the carbides and having the same impact.

The effect of duration can be considered to have the same impact as feed sizes, as it varies the end particle size distribution as the rocks are crushed. This was shown in all abrasive types.

Previously it was thought that the benefit would be improved with smaller particle size, but the reverse of that trend was observed under tested conditions. This suggests a critical particle size where benefit in greater below and worsens after. As final particle size was not measured it is difficult to conclude if this is the case but given the feed particle sizes are larger than the standard 6.7mm for complete crushing in the BMAT.

Further, in conditions of medium or coarse PSD for short duration in every abrasive type, it was noted that some rounds pebbles were present at the end of testing which is not ideal as when the abrasive is broken up it allows for fresh cutting edges to continue the abrasive wear

5.2 Alloy Parameters

5.2.1 Carbide Volume Fraction

When looking generally the CVF was shown to not have a direct correlation to wear life in the conditions tested. The same tend of the low Cr:C series to show approximately level wear rates across the range of CVF tested. In the high Cr: C series the trend showed a maximum level of wear approximately 25 vol% with lower wear rates seen either side. However this series is the smallest with only six alloys, the alloy with the least CVF often performs the best with the 2nd and 3rd lowest having the worst performance. Finally medium Cr:C shows the clearest trend of improving to around 30 vol% then detrimental beyond this point.

Further testing is required to determine why CVF does not have a direct correlation to wear life in the conditions tested, as was initially thought with a larger presence of the harder phase, wear life would be increased however this was not the case in the high stress abrasion conditions present.

LS-35 chipped on multiple occasions but in two tests both blocks chipped leading to it being excluded from those tests results. This is partly due to only being 2 blocks of this specific specimen unlike the average of 5 blocks.

The predicted existence of a critical particle size would also explain why CVF does not have a proportional benefit when increase, as initially expected.

As found by Chen, CVF and Cr:C had more of an impact in low stress abrasion than in high. The wear conditions of the BMAT test completed are all high stress abrasion and no clear correlation was shown. This concurs with the findings of Gates, et al in the Osaka project. When the results are compared from test to test, similar patterns are displayed. This implies that while these parameters are not showing clear trends, the properties of the specimens in these conditions may be dependent on another variable not tested.

5.2.2 Chromium to carbon ratio

The effect of Cr:C shows a consistent trend whereby wear life is reduced with increasing Cr:C. This was as predicted since increasing the Cr:C leads to softer materials. In most tests, it can be observed that the trend of the high CVF performs better than the low CVF at low Cr:C, and low CVF perform better in higher CVF. The graphs plotting wear rate against Cr:C show wear rates for low (4.9 – 6.8), medium (6.8 – 7.9) and high (9.2 – 10.8) Cr:C are observed to be in increasing order, implying an increase in Cr:C leads to an increase in wear rate. Between low and medium levels, only slightly higher wear rates were noted, however for high range, the detrimental effect is clear.

The decrease in hardness is attributed to the method of changing the Cr:C. The ratio is increased by either: lowering the carbon content while chromium is held constant, or by increasing the chromium while holding the carbon constant. By decreasing the carbon, carbon becomes a limiting factor in formation of the carbide phases. Further for the matrix, tetragonality of the martensitic matrix increases with carbon content, which in turn increases hardness and strength (Lobodyuk, Meshkov, & Pereloma, 2019).

By increase the chromium content, carbon is consumed in the formation of carbides, leaving less retained carbon in the matrix, also impacting tetragonality. The increase of chromium leads to a decrease of the carbon content of the matrix (Laird, Gundlach, & Rohrig, 2000). So either an increase in chromium or a decrease in carbon can impact the hardness.

Despite the decrease of hardness, the chromium benefits corrosion resistance, therefore a balance between wear life and corrosion could be made. The benefit to corrosion resistance was also observed after each test, where the white cast irons had much less visible evidence of corrosion than the steels.

However, on the graphs plotting wear rate against CVF, a trend more typical of Cr:C was found when comparing the trendlines. The benefit should increase to a critical point then decrease, as observed on the CVF graph trendlines. Consistently, performance was best in medium, followed by low, then high. This appears contrary to the findings of the Cr:C graphs. This a clear trend in the low and medium CVF range and breaks down beyond ~36 vol%. This is in part due to the grouping of the CVF series, and how Cr:C is not held perfectly constant (±1). There is scatter of results, even within the same series, with marginally different CVF, implying the trendlines are not highly accurate.

5.3 Replicate Tests

The replicates of granite, medium, short and granite, coarse, long produced results within statistical scatter implying these tests were repeatable. However the replicate of the basalt, coarse, short test yielded results that varied from the original test. Comparing the size of error bar in Figure 12 and Figure 13 to Figure 14 and Figure 15, it was shown that the induvial specimen types had larger error hence this test was excluded from the benefit ratio representation. A possible reason for this large difference is the basalt used in the 2 tests may have been from two separate crushing sessions, with rock sources months apart. Meaning the composition of the rock may be slightly different and the PSD while in the same range may not have the same scatter between 13.2mm and 9.5mm as a different crusher gap was used.

6.0 Conclusion

The evaluation of the effect of alloy parameters and testing conditions produced results inconsistent with those initially expected.

Past testing methodology seen in the literature review was noted to not be a realistic representation of industrial wear conditions. Further, a knowledge gap of the exact effects of CVF and Cr:C was determined.

The BMAT was implemented under selected testing conditions to determine the impacts of abrasive type, feed particle size distribution and duration. Specimens with systematically varied CVF and Cr:C were implemented to determine the impacts of these alloy parameters

The testing determined that:

(1) The magnitude of benefit of white cast irons compared to low-alloy steels is largest when tested in softer abrasives. This is consistent with past publications.

(2) For a given abrasive rock type, the magnitude of benefit of white cast irons was greater for larger feed particle size. This is contrary to the findings of past experimental work.

(3) Carbide volume fraction did not show a clear effect on wear performance. This is reasonably consistent with past work, which has shown only weak (and somewhat variable) effects of CVF on abrasion performance under high stress abrasion conditions.

(4) Increasing chromium to carbon ratio was found to have a negative effect on abrasive wear life, although it may benefit corrosion resistance.

(5) An alloy denoted Y062 (medium range CVF of 34.6 vol% and the medium Cr:C ratio of 5.3) showed the best wear performance averaged over all wear conditions.

7.0 Recommendations

Recommendations for future testing include more testing with BMAT with gaps between particle size distribution to highlight the effect of sized. Alternatively, within these distributions ensuring fair spread of sizes as the makeup within these ranges as it was not exactly known.

Further consideration of different methods of Normalization, such as by surface area could be used. This was briefly explored in testing but only done for a limited range of specimens due to time constraints.

The aim of the normalization method investigation is to develop a normalization method that provides a lower scatter from the average of data points within an individual specimen types. Appendix A: Normalization Method explores the benefits of different normalization methods. To show the viability of these various methods and make recommendation on the normalization method to be used for future testing. Normalizing by both initial weight and surface area overcompensates for initial conditions therefore was not plotted and the others were focused on.

Normalizing by surface area over initial weight provides tighter scatter of the data around average in the majority of conditions tested. However these benefits are fairly marginal. I is recommend to take area data for smaller sample sets however for large sets as it is time consuming for measurement it is not recommended for marginal benefits.

References

Archard, J. F., & Hirst, W. (1956). The Wear of Metals under Unlubricated Conditions. In *Proceedings of the Royal Society of London. Series A, Mathematical and Physical Sciences (1934-1990), 236(1206)* (pp. 397- 410). Royal Society.

Chen, T. (2018). *Performance Benchmarking for NiHard Ore Chute Liner Alloys – Ball Mill Abrasion Test & Rubber Wheel Abrasion Test.* n.p.

Comino, A. (2009). *Effect of "Impact" on the Performance of White Cast Irons Relative to Low-Alloy Steels in Grinding Mills.*

Gates, J. D., & Gore, G. J. (1995). Wear of Materials: Philosophies and Practicalities. In *Materials Fourm, 19* (pp. 53-89). St Lucia, QLD: Department of Mining and Metallurgical Engineering , University of Queensland.

Gates, J., Bennet, P., Pourasiabi, H., Demirer, E., Comino, A., Keen, L., & Knibbe, R. (2017). Understanding the Performance of Abrasion-resistant High-Cr White Cast Irons in Terms of Micro-, Meso- and Macro-scale Fracture Mechanisms . *6th International Conference on Abrasion Wear Resistant Alloyed White Cast Iron for Rolling and Pulverizing Mills* (pp. 1-19). Brisbane: School of Mechanical and Mining Engineering, The University of Queensland.

Gates, J., Dargusch, M., Walsh, J., Field, S., Hermand, M.-P., Delaup, B., & Saad, J. (2008). Effect of abrasive mineral on alloy performance in. *Wear, 265*, 865–870.

Hamzah, M. H. (2018). *Performance Benchmarking for Ni-Hard Ore Chute Liner Alloy BMECT and BMAT.*

Heino, V., Kallio, M., Valtonen, K., & Kuokkala, V.-T. (2017). The role of microstructure in high stress abrasion of white cast irons. *Wear*, 119-125.

Hutchings, I., & Shipway, P. (2017). *Friction and Wear of Engineering Materials.* Elsevier.

Jankovic, A., Wills, T., & Dikmen, S. (2016). A Comparison of Wear Rates of Ball Mill Grinding Media. *Journal of Mining and Metallurgy, 52 A*, 1-10.

Laird, G., Gundlach, R., & Rohrig, K. (2000). *Abrasion-Resistant Cast Iron Handbook* . Schaumburg: American Foundary Society.

Littler, J. (2015). *Effect of Mill Operating Parameter on Absolute and Relative Performance of Low-Alloy Steel and High-Cr White Cast Iron Grinding Balls –Abrasive Wear*.

Lobodyuk, v., Meshkov, Y., & Pereloma, E. (2019). On Tetragonality of the Martensite Crystal Lattice in Steels. *Metallurgical and Materials Transactions A, 50*, 97-103.

Marnane, W. (2018). Performance Benchmarking for Ni-Hard Ore Chute Liner Alloys—ICAT and RWAT.

Peng, Y.-X., Ni, X., Zhu, Z.-C., Yu, Z.-F., Yin, Z.-X., Li, T.-Q., . . . Xu, J. (2017). Friction and wear of liner and grinding ball in iron ore ball mill. *Tribology International*, 506-517.

Zum Gahr, K.-H. (1987). *Microstructure and Wear of Materials.* Siegen: Elsevier.

Appendix

Appendix A: Normalization Method

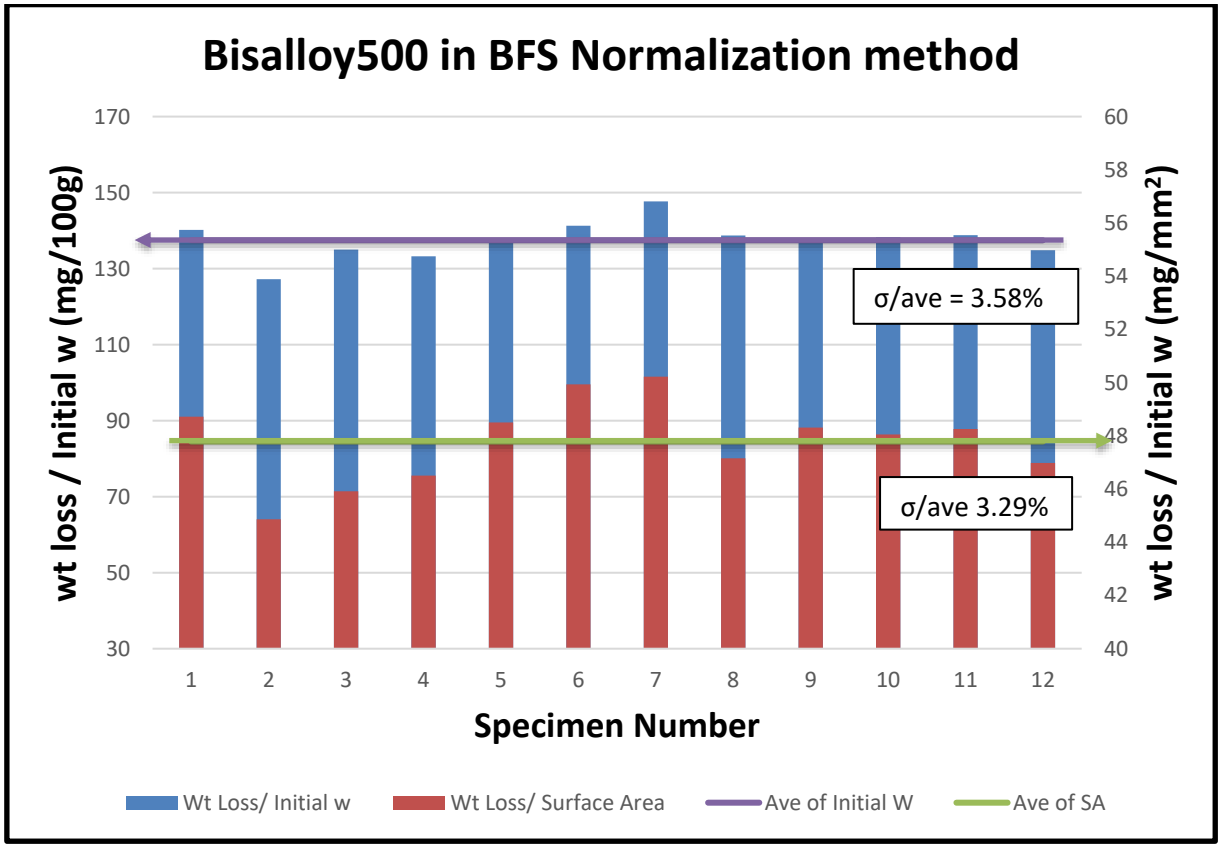

Figure 37: Bisalloy500 in Basalt, Fine, Short comparing Normalization method

Table 7: Bisalloy500 in Basalt, Fine, Short comparing Normalization method

	Initial W	*Surface area*	*Initial W and SA*
STDEV	4.92	1.57	12.11
Average	137.45	47.79	257.22
STDEV/Average	3.58%	3.29%	4.71%

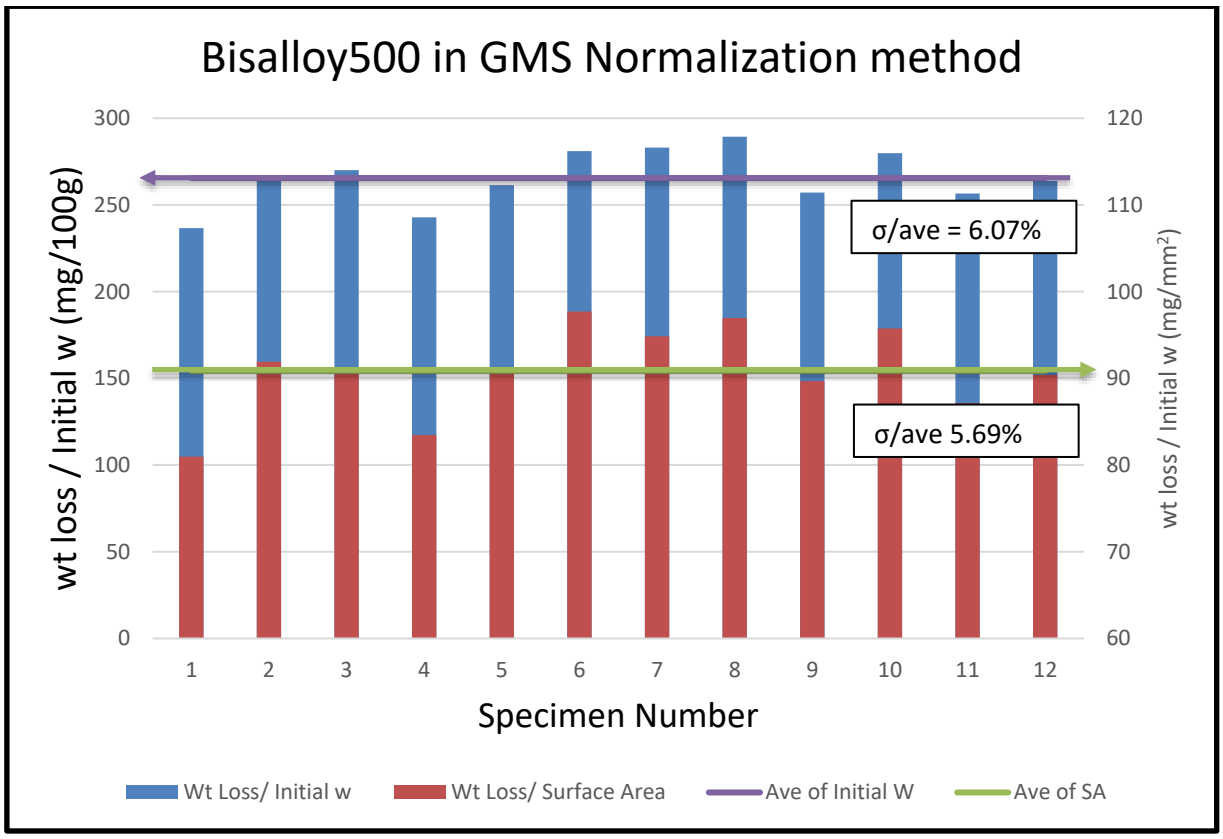

Figure 38: Bisalloy500 in Granite, Medium, Short comparing Normalization method

Table 8: Bisalloy500 in Granite, Medium, Short comparing Normalization method

	Initial W	*Surface area*	*Initial W and SA*
STDEV	16.12	5.17	35.69
Average	265.49	90.86	502.85
STDEV/Average	6.07%	5.69%	7.10%

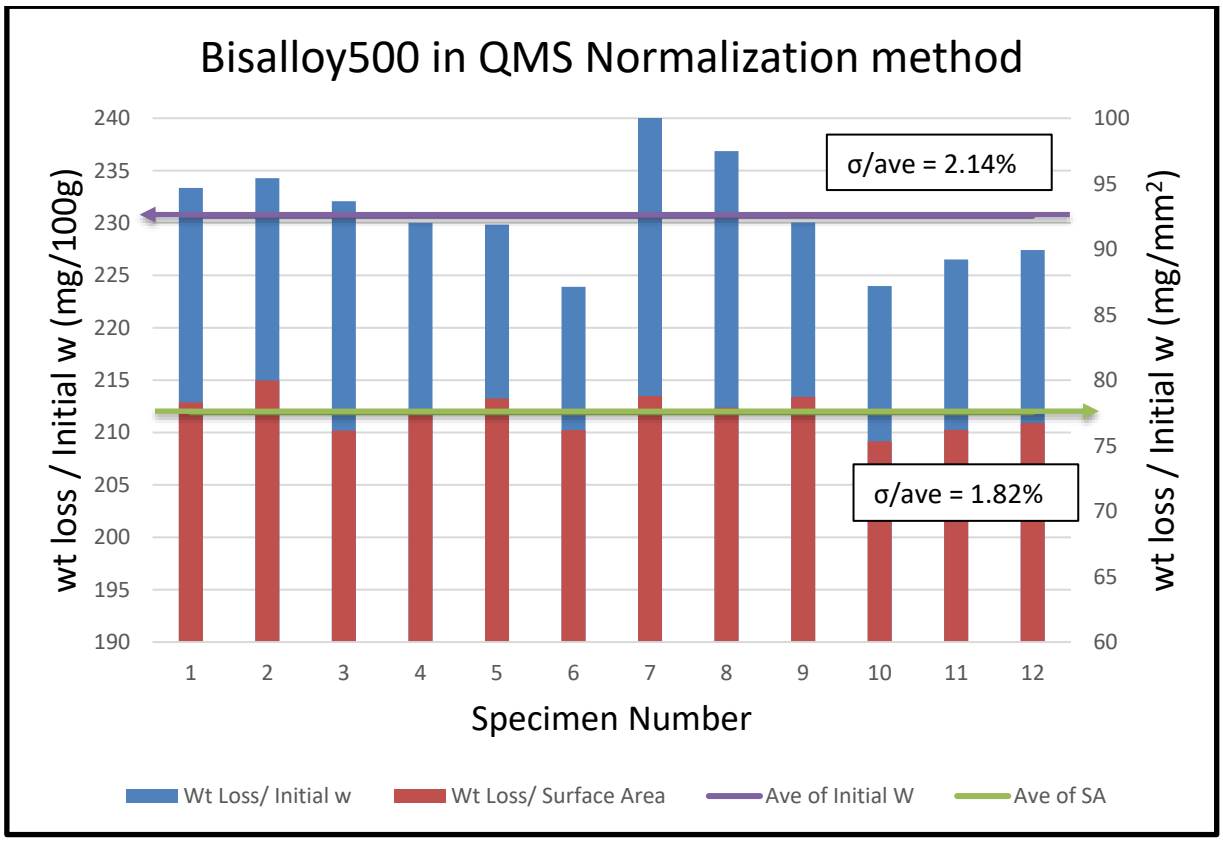

Figure 39: Bisalloy500 in Quartzite, Medium, Short comparing Normalization method

Table 9: Bisalloy500 in Quartzite, Medium, Short comparing Normalization method

	Initial W	*Surface area*	*Initial W and SA*
STDEV	4.94	1.41	16.20
Average	230.70	77.55	441.63
STDEV/Average	2.14%	1.82%	3.67%

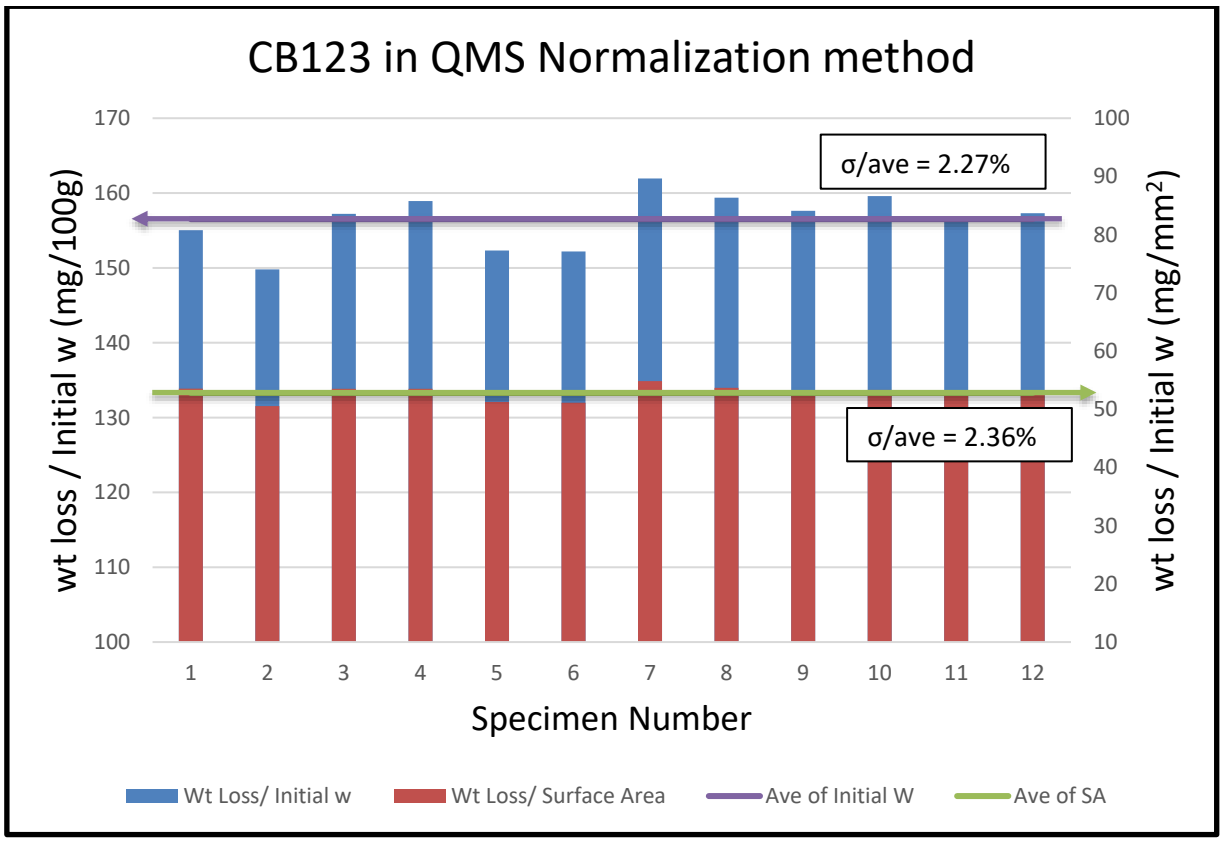

Figure 40: CB123 in Quartzite, Medium, Short comparing Normalization method

Table 10: CB123 in Quartzite, Medium, Short comparing Normalization method

	Initial W	*Surface area*	*Initial W and SA*
STDEV	3.56	1.25	6.87
Average	156.51	52.79	280.29
STDEV/Average	2.27%	2.36%	2.45%

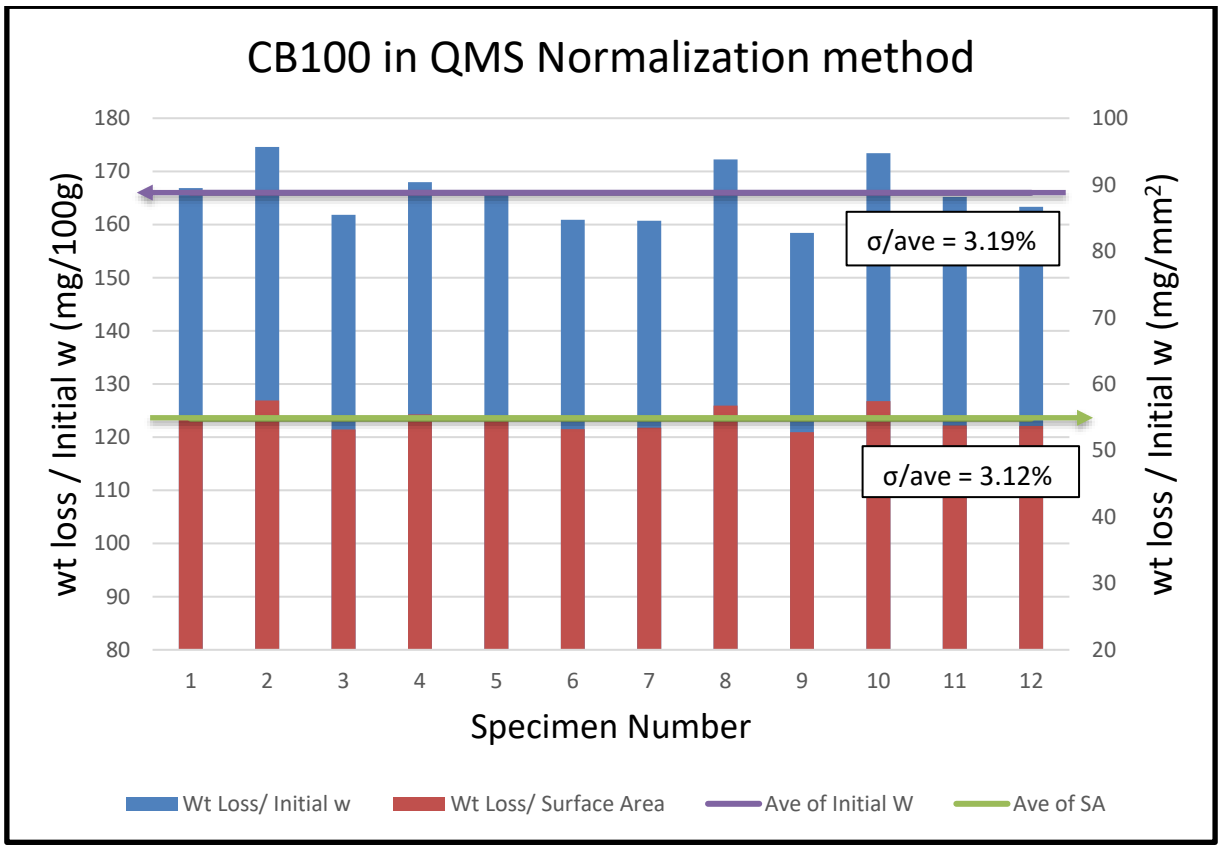

Figure 41: CB100 in Quartzite, Medium, Short comparing Normalization method

Table 11: CB100 in Quartzite, Medium, Short comparing Normalization method

	Initial W	*Surface area*	*Initial W and SA*
STDEV	5.30	1.71	10.34
Average	165.97	54.77	300.73
STDEV/Average	3.19%	3.12%	3.44%

Appendix B: Full List of Samples with Labels and Chemical Compositions

Table 12: Sample List

X-code	**Y-code**				**Chemical Composition**								
	CB-Code	**Labels**	**CVF(E)**	**CrE:C**	**C**	**Cr**	**Mo**	**Cu**	**Mn**	**Si**	**Ni**	**W**	**V**
A05	**CB097**	**97_**	34.4	9.2	2.85	27.00	0.00	0.00	2.00	0.50	0.00	0.00	0.00
CB100	**CB100**	**100_**	42.6	5.9	3.71	22.01	0.97	0.00	1.07	0.39	0.94	0.00	0.00
NbCVF.M-00	**CB123**	**123_**	15.6	10.4	1.71	17.94	0.87	0.02	0.74	0.31	0.75	0.00	0.00
Oregon	**LS-25**	**25_**	16.6	10.8	1.76	18.10	1.82	1.11	1.09	1.28	1.50	0.00	0.00
Oregon	**LS-28**	**28_**	16.3	8.3	1.89	14.64	1.86	0.53	1.04	1.22	1.47	0.00	0.00
Oregon Good	**LS-35**	**35_**	14.6	6.9	1.87	11.95	1.93	1.01	1.14	0.50	1.18	0.00	0.00
Oregon Best	**LS-36**	**36_**	16.5	9.8	1.81	17.21	1.02	1.02	1.17	1.30	1.88	0.00	0.00
CVF22-BS	**Y002**	**2_**	22.0	7.0	2.30	16.53	0.52	0.56	0.92	0.79	0.46	0.00	0.00
CVF25-BS	**Y003**	**3_**	25.2	7.5	2.45	18.86	0.51	0.90	0.97	0.73	0.46	0.00	0.00
CVF42-BS	**Y006**	**6_**	41.8	7.6	3.46	26.52	0.49	0.97	0.77	0.73	0.49	0.00	0.00
CVF17-BS	**Y007**	**7_**	16.6	7.7	1.92	15.14	0.52	0.93	0.67	0.69	0.45	0.00	0.00
CVF36-BS	**Y008**	**8_**	36.1	7.4	3.13	23.56	0.48	0.14	2.06	0.70	0.18	0.00	0.00
Cr/C08-BS	**Y017**	**17_**	34.5	7.8	3.00	23.64	0.47	0.78	0.92	0.83	0.33	0.00	0.00
Cr/C10-BS	**Y018**	**18_**	34.1	9.7	2.79	27.49	0.50	0.78	0.88	0.94	0.32	0.00	0.00
Cr/C03-BS	**Y019**	**19_**	31.8	3.4	3.31	11.41	1.03	0.70	0.98	0.83	0.31	0.00	0.00
Ni00-BS	**Y030**	**30_**	33.5	7.0	3.01	21.51	0.47	0.76	0.76	0.85	0.21	0.00	0.00
Si05-BS	**Y034**	**34_**	33.7	6.8	3.05	21.03	0.50	0.81	0.89	0.54	0.36	0.00	0.00
CVF40-BS	**Y037**	**37_**	40.3	6.9	3.45	24.04	0.51	0.86	0.80	0.83	0.37	0.00	0.00
ML3	**Y038,57,65,74**	**57_**	28.2	7.9	2.71	20.60	0.62	0.86	0.88	0.75	0.25	0.00	0.00
Cr/C07-BS	**Y040**	**40_**	32.3	7.1	2.93	21.10	0.48	0.80	0.68	0.82	0.35	0.00	0.00
Cu13-BD	**Y041**	**41_**	32.6	5.1	3.16	16.11	1.21	1.27	0.82	0.74	0.25	0.00	0.00
BB4	**Y042,43,82,83,86**	**43_**	31.8	5.5	3.06	16.86	1.16	0.89	1.10	0.74	0.26	0.00	0.00

ML4	**Y047**	**47_**	20.1	9.7	2.06	19.16	0.00	1.35	1.14	0.88	0.22	0.00	0.00
Cu03-BD	**Y050**	**50_**	33.4	5.0	3.22	16.24	1.19	0.41	0.81	0.79	0.25	0.00	0.00
CVF30-BD	**Y054**	**54_**	29.5	4.9	2.98	14.54	1.18	0.94	0.77	0.68	0.25	0.00	0.00
Cr/C060-BD	**Y055**	**55_**	33.8	5.8	3.16	18.45	1.23	0.94	0.82	0.78	0.35	0.00	0.00
CVF38-BD	**Y056**	**56_**	37.8	5.0	3.51	17.80	0.89	0.92	0.82	0.76	0.27	0.00	0.00
CVF24-BD	**Y059**	**59_**	24.4	4.9	2.64	12.91	1.21	0.92	0.89	0.71	0.25	0.00	0.00
Cr/C055-BD	**Y062**	**62_**	34.6	5.3	3.26	17.45	1.22	0.95	0.81	0.75	0.27	0.00	0.00
CVF34-BD	**Y066**	**66_**	34.1	4.9	3.28	16.17	1.24	0.94	0.80	0.71	0.26	0.00	0.00
CVF19-BD	**Y070**	**70_**	18.7	5.0	2.25	11.21	1.27	0.93	0.77	0.63	0.24	0.00	0.00
CVF42-BD	**Y071**	**71_**	41.7	5.1	3.76	19.23	1.16	0.89	0.83	0.76	0.27	0.00	0.00
CVF18-BD	**Y072**	**72_**	17.9	5.1	2.19	11.22	1.29	0.94	1.09	0.33	0.24	0.00	0.00
Cr/C040-BD	**Y073**	**73_**	30.9	4.3	3.15	13.36	1.27	0.79	0.87	0.67	0.28	0.00	0.00
ARNE	**A20,26**	**A20_A26_**	-	-	0.95	0.60	0.00	0.00	1.10	0.00	0.00	0.60	0.10
BK245	**B14,20,26**	**B14_ B20_ B26_**	-	-	0.63	0.60	0.00	0.00	1.10	1.10	0.00	0.00	0.00

Appendix C: Hardness Data

Table 13: Hardness Data

Alloy Code	**Sample**	**Hardness Measurements**										**VHN**	**VHN**	**Normalized**
X-, Y-, CB-, JR-, A-, B-	**Label**	**1st**	**2nd**	**3rd**	**4th**	**5th**	**6th**	**7th**	**8th**	**9th**	**10th**	**Average**	**STDEV**	**STDEV %**
CB097	**97_1**	817.6	786.8	778.9	803.1	767.1	773.1	804.6	764.5	768.2	777.5	784	18	2.3%
CB100	**100_2**	836.4	853.2	847.2	844.3	840.3	820.1	831.3	833.5	852.5	868.4	843	14	1.6%
CB123	**123_3**	739.4	738.3	727.7	704.6	724.8	707.6	731.1	723.0	732.4	722.2	725	12	1.6%
LS-25	**25_3**	687.8	671.7	671.4	657.6	686.6	663.6	667.9	670.5	666.1	688.8	673	11	1.6%
LS-28	**28_3**	706.6	688.8	686.8	712.6	738.6	697.3	680.6	699.8	708.8	709.1	703	17	2.3%
LS-35	**35_2**	581.7	570.8	607.4	606.2	578.0	591.8	578.0	566.2	616.1	595.7	589	17	2.9%
LS-36	**36_2**	679.7	690.2	701.8	704.3	713.4	692.4	702.5	698.3	697.6	710.1	699	10	1.4%
Y002	**2_1**	776.9	747.8	759.5	755.6	811.7	804.0	770.8	797.9	792.2	789.2	781	22	2.8%
Y003	**3_2**	840.0	815.7	819.5	833.5	846.2	831.9	841.0	820.1	816.4	823.0	829	11	1.4%
Y006	**6_3**	810.8	816.7	827.4	835.1	860.3	863.7	820.7	840.3	828.7	821.1	832	18	2.1%
Y007	**7_2**	751.7	744.8	738.6	738.3	772.3	742.9	753.3	748.4	735.4	757.8	748	11	1.5%
Y008	**8_3**	832.2	792.2	820.1	833.8	815.7	819.8	823.9	821.7	813.2	845.2	822	14	1.7%
Y017	**17_2**	872.9	862.0	842.3	818.9	845.6	866.4	852.9	845.9	869.8	859.3	854	16	1.9%
Y018	**18_2**	831.6	802.2	791.0	835.1	790.7	789.8	793.7	788.6	795.2	769.4	799	20	2.5%
Y019	**19_2**	809.8	801.2	758.6	823.9	771.1	799.1	775.1	799.1	760.3	810.4	791	23	2.9%
Y030	**30_3**	826.5	848.5	842.9	841.6	842.9	862.6	865.0	852.2	881.6	823.9	849	18	2.1%
Y034	**34_2**	846.9	843.9	852.5	849.2	840.0	859.6	871.5	853.2	864.7	852.5	853	10	1.1%
Y037	**37_1**	859.6	874.7	865.4	868.1	911.5	858.6	855.2	845.2	852.9	867.8	866	18	2.1%
Y057	**57_2**	797.0	803.4	783.9	783.9	775.7	824.5	808.0	805.2	814.2	756.4	795	20	2.5%
Y040	**40_3**	812.9	822.0	809.5	844.6	835.4	842.6	834.5	814.8	840.6	838.0	829	13	1.6%
Y041	**41_3**	784.5	778.9	804.3	803.1	819.5	830.0	805.5	828.4	825.2	816.0	810	18	2.2%

Y043	**43_3**	807.7	834.8	765.1	800.6	792.2	826.2	808.0	803.7	815.1	779.8	803	21	2.6%
Y047	**47_2**	709.8	669.3	671.4	708.6	718.3	716.0	717.8	696.8	700.8	717.8	703	19	2.6%
Y050	**50_2**	872.9	863.0	853.2	890.5	869.8	877.8	838.7	865.0	881.6	882.3	869	15	1.8%
Y054	**54_3**	781.3	793.4	788.3	776.3	800.3	797.0	793.1	819.8	801.9	784.5	794	12	1.6%
Y055	**55_3**	844.3	862.6	845.9	851.9	842.0	813.9	855.2	866.7	826.8	853.9	846	16	1.9%
Y056	**56_2**	834.8	818.2	830.0	807.7	837.4	813.9	829.3	835.8	828.4	820.1	826	10	1.2%
Y059	**59_3**	776.0	749.2	737.8	758.9	764.8	797.3	741.8	755.0	769.1	753.9	760	17	2.3%
Y062	**62_1**	836.7	787.7	786.5	810.1	791.9	802.2	818.9	797.9	829.0	795.8	806	17	2.2%
Y066	**66_1**	857.9	824.9	807.1	797.0	809.5	788.6	807.1	780.1	835.1	830.3	814	23	2.9%
Y070	**70_2**	661.0	693.9	692.2	663.8	705.6	674.5	681.8	659.2	694.9	689.0	682	16	2.4%
Y071	**71_2**	864.0	850.5	876.4	847.2	823.3	832.9	878.5	880.6	877.8	826.1	856	23	2.7%
Y072	**72_2**	565.0	553.3	582.8	566.8	577.2	579.5	573.3	584.2	565.7	560.8	571	10	1.8%
Y073	**73_1**	842.0	825.5	806.4	802.8	801.2	821.7	807.7	828.7	841.3	799.1	818	16	2.0%
JR	**JR_1**	563.5	583.4	578.3	580.6	590.3	597.4	592.2	579.1	577.0	602.4	584	11	1.9%
A20	**A20_**	722.7	722.4	742.9	734.6	742.1	745.1	744.8	731.9	723.0	730.3	734	9	1.3%
A26	**A26_**	709.1	692.9	704.8	709.6	708.3	694.9	698.3	697.6	707.6	696.6	702	7	0.9%
B14	**B14_**	773.1	762.8	750.8	731.4	759.5	744.0	763.1	745.4	750.0	735.4	752	13	1.7%
B20	**B20_**	698.8	681.4	698.8	692.7	692.9	686.8	681.8	693.9	695.9	702.5	693	7	1.0%
B26	**B26_**	693.6	685.6	675.2	674.0	672.4	695.9	671.0	670.3	682.3	675.4	680	9	1.4%